Please cite this article in press as: Xie et al., NAC1 regulates root ground tissue maturation by coordinating with the SCR/SHR–CYCD6;1 module in *Arabidopsis*, Molecular Plant (2023), https://doi.org/10.1016/j.molp.2023.02.006

Molecular Plant
Research article

CellPress
Partner Journal

NAC1 regulates root ground tissue maturation by coordinating with the SCR/SHR–CYCD6;1 module in *Arabidopsis*

Chuantian Xie[1], Cuiling Li[1], Fengxia Wang[1], Feng Zhang[1], Jiajia Liu[1], Junxia Wang[1], Xiansheng Zhang[2], Xiangpei Kong[1,*] and Zhaojun Ding[1,*]

[1]The Key Laboratory of Plant Development and Environmental Adaptation Biology, Ministry of Education, College of Life Sciences, Shandong University, Qingdao, Shandong 266237, China

[2]National Key Laboratory of Crop Biology, College of Life Sciences, Shandong Agricultural University, Taian, Shandong 271018, China

***Correspondence: Xiangpei Kong (kongxiangpei@sdu.edu.cn), Zhaojun Ding (dingzhaojun@sdu.edu.cn)**

https://doi.org/10.1016/j.molp.2023.02.006

ABSTRACT

Precise spatiotemporal control of the timing and extent of asymmetric cell divisions (ACDs) is essential for plant development. In the *Arabidopsis* root, ground tissue maturation involves an additional ACD of the endodermis that maintains the inner cell layer as the endodermis and generates the middle cortex to the outside. Through regulation of the cell cycle regulator *CYCLIND6;1* (*CYCD6;1*), the transcription factors SCARECROW (SCR) and SHORT-ROOT (SHR) play critical roles in this process. In the present study, we found that loss of function of *NAC1*, a NAC transcription factor family gene, causes markedly increased periclinal cell divisions in the root endodermis. Importantly, NAC1 directly represses the transcription of *CYCD6;1* by recruiting the co-repressor TOPLESS (TPL), creating a fine-tuned mechanism to maintain proper root ground tissue patterning by limiting production of middle cortex cells. Biochemical and genetic analyses further showed that NAC1 physically interacts with SCR and SHR to restrict excessive periclinal cell divisions in the endodermis during root middle cortex formation. Although NAC1–TPL is recruited to the *CYCD6;1* promoter and represses its transcription in an SCR-dependent manner, NAC1 and SHR antagonize each other to regulate the expression of *CYCD6;1*. Collectively, our study provides mechanistic insights into how the NAC1–TPL module integrates with the master transcriptional regulators SCR and SHR to control root ground tissue patterning by fine-tuning spatiotemporal expression of *CYCD6;1* in *Arabidopsis*.

Key words: root, NAC1, SCR, SHR, TOPLESS, CYCD6;1

Xie C., Li C., Wang F., Zhang F., Liu J., Wang J., Zhang X., Kong X., and Ding Z. (2023). NAC1 regulates root ground tissue maturation by coordinating with the SCR/SHR–CYCD6;1 module in *Arabidopsis*. Mol. Plant. **16**, 1–17.

INTRODUCTION

In plants as in animals, growth and development rely on a continuous supply of specialized cells derived from stem cells (Scheres, 2007; Dinneny and Benfey, 2008). Asymmetric cell divisions (ACDs) must be precisely coordinated with cell differentiation to generate daughters with distinct fates (Ten Hove and Heidstra, 2008; Abrash and Bergmann, 2009; Boyer and Simon, 2015). This coordination is essential for proper tissue patterning and function.

Plant stem cells and their niches are located within the shoot and root meristems (Dinneny and Benfey, 2008; Aichinger et al., 2012). The root meristem contains four types of tissue-specific stem cells, and the cortex/endodermal stem cells generate the ground tissues, which are composed of the endodermis and cortex (Benfey and Scheres, 2000). The cortex/endodermal stem cells undergo two stereotypical and successive ACDs to establish and maintain the ground tissues: the cortex/endodermis initial (CEI) cell undergoes an anticlinal division that generates a new CEI cell and a CEI daughter (CEID) cell; the CEID cell then undergoes a single periclinal division to give rise to an inner daughter cell that generates the endodermis and an outer daughter cell that generates the cortex (Dinneny and Benfey, 2008; Scheres, 2007; van den Berg et al., 1995; van den Berg et al., 1997). By 7–14 days post germination (dpg),

Published by the Molecular Plant Shanghai Editorial Office in association with Cell Press, an imprint of Elsevier Inc., on behalf of CSPB and CEMPS, CAS.

Please cite this article in press as: Xie et al., NAC1 regulates root ground tissue maturation by coordinating with the SCR/SHR–CYCD6;1 module in *Arabidopsis*, Molecular Plant (2023), https://doi.org/10.1016/j.molp.2023.02.006

the third layer of ground tissues, termed the middle cortex, is formed in the endodermis via periclinal ACD. Therefore, the production of middle cortex cells is considered to be an indicator of root ground tissue maturation (Baum et al., 2002; Paquette and Benfey, 2005; Cui and Benfey, 2009a, 2009b; Heo et al., 2011; Koizumi et al., 2012a, 2012b; Pauluzzi et al., 2012).

Proper patterning of the root ground tissues requires the SCARECROW (SCR)/SHORT- ROOT (SHR) transcription factor complex. *SHR* is transcriptionally expressed in the stele, and its encoded protein moves to the outer adjacent cell layer, where SCR sequesters SHR to the nucleus by forming an SHR/SCR complex (Gallagher et al., 2004; Cui et al., 2007). This complex orchestrates a transcriptional program by promoting transcription of a key component of the cell cycle machinery, *CYCLIND6;1* (*CYCD6;1*), specifically in CEI and CEID cells (Sozzani et al., 2010; Koizumi et al., 2012b; Cruz-Ramírez et al., 2012). A local increase in auxin levels in the endodermis is critical for generating new ACDs through induction of *CYCD6;1* expression, which requires SHR and SCR activity (Cruz-Ramírez et al., 2012). During root middle cortex formation, SCR plays a negative role by suppressing *CYCD6;1* expression (Paquette and Benfey, 2005; Koizumi et al., 2012b). However, periclinal cell division fails to take place in the *shr* mutant, which might be a result of the absence of the endodermis when *SHR* is mutated (Paquette and Benfey, 2005). All of these results suggest a complex interaction between SCR and SHR during root ground tissue formation (Paquette and Benfey, 2005; Cui and Benfey, 2009a, 2009b; Heo et al., 2011; Koizumi et al., 2012b).

Root middle cortex formation is significantly reduced in the *cycd6;1* mutant, and it is lost entirely in the *shr-2* mutant (Paquette and Benfey, 2005; Sozzani et al., 2010). In *scr-5* mutants, the root middle cortex forms earlier than in the wild type (WT) (Paquette and Benfey, 2005). Notably, the amount of SHR in the endodermis controls when and where the middle cortex forms; when SHR is maintained at high levels in the endodermis, periclinal cell divisions are inhibited, whereas a decrease in SHR promotes expression of *CYCD6;1* and, therefore, middle cortex formation in the root (Koizumi et al., 2012b). Another GAI, RGA and SCR (GRAS) transcription factor, SCR-LIKE 3 (SCL3), acts downstream of DELLA transcription factors; it is downregulated by gibberellic acid (GA) and upregulated by the SHR/SCR complex (Heo et al., 2011; Zhang et al., 2011). In addition, similar to the *scr-5* mutant, the *scl3* mutant shows premature root middle cortex formation, whereas overexpression of *SCL3* suppresses periclinal ACDs in the endodermis. SEUSS, a transcription factor that acts upstream of SHR, SCR, and SCL3, integrates the SHR/SCR pathway and GA signaling to regulate middle cortex formation in the *Arabidopsis* root (Gong et al., 2016). A time-dependent threshold of the transcription factor PHABULOSA governs the timing of root middle cortex formation by controlling GA homeostasis and *CYCD6;1* expression in the endodermis (Bertolotti et al., 2021).

Regulation of transcription is central to many biological processes. It involves transcription factors that bind to regulatory sequences and either activate or repress gene expression. For repression, eukaryotes have developed various strategies involving proteins known as co-repressors (Payankaulam et al., 2010). Many studies show that the repressive function of these factors in plants involves direct interaction with the co-repressor TOPLESS (TPL) (Causier et al., 2012). TPL and four other TPL-RELATED (TPR) homologs belong to the family of Groucho/Tup 1 transcriptional co-repressors (Long et al., 2006) that bind to a wide range of transcription factors via their ethylene response factor–associated amphiphilic repression (EAR) motifs to repress downstream targets (Kagale and Rozwadowski, 2011; Causier et al., 2012).

Petunia no apical meristem and *Arabidopsis* transcription activation factor 1 (ATAF1), ATAF2, and CUP-SHAPED COTYLEDONS 2 (NAC) domain proteins comprise a large, plant-specific family of transcription factors involved in many aspects of plant development (Kikuchi et al., 2000; Riechmann et al., 2000; Hegedus et al., 2003; Ooka et al., 2003). The NAC domain was originally characterized in petunia no apical meristem and in ATAF1, ATAF2, and CUP-SHAPED COTYLEDONS (Aida et al., 1997). The NAC family gene NAC1 promotes lateral root development by transducing auxin signals downstream of the F-box protein TIR1 (Xie et al., 2000). More recently, NAC1 has been reported to regulate primary root growth by directly repressing transcription of *E2 promoter-binding factor a* (Xie and Ding, 2022). NAC family proteins have also been shown to regulate cell division in shoot stem cells (Abrash and Bergmann, 2009).

Here we report that NAC1 coordinates with SCR and SHR to control the precise periclinal ACDs of the endodermis during root middle cortex formation. We demonstrate that NAC1, acting as a negative regulator, interacts with the co-repressor TPL to directly repress transcription of *CYCD6;1* in this process. In addition, we show that NAC1 genetically and physically interacts with the master regulators SCR and SHR to restrict excessive periclinal cell divisions in the endodermis to form middle cortex cells by finely tuning the spatiotemporal expression of *CYCD6;1*.

RESULTS

Knockdown of *NAC1* causes excessive periclinal cell divisions of the endodermis

We performed β-glucuronidase (GUS) staining analysis with a translational fusion to the GUS reporter line (*NAC1pro:gNAC1-GUS*) and observed high expression of NAC1 in ground tissue (Supplemental Figure 1), prompting us to investigate its role in root ground tissue patterning. For this purpose, we obtained two *Arabidopsis* transfer DNA (T-DNA) insertion *NAC1* mutant lines (*Salk_098992*, *nac1-1* and *Salk_052190*, *nac1-2*), which showed reduced abundance of *NAC1* transcripts (Supplemental Figure 2A and 2B). We also generated *NAC1* overexpression transgenic lines by overexpressing a mutant version of *mNAC1* (*35S::MYC-mNAC1*, *mNAC1ox*) with a disrupted miR164 binding site (Supplemental Figure 2C and 2D).

In WT roots, the CEI cell divides anticlinally and generates the CEID cell, which undergoes periclinal ACD and generates endodermis and cortex cell layers (Supplemental Figure 3A and 3B). Although the transcriptional reporter *CYCD6;1pro:GFP*, which is specifically expressed in the CEI cells and CEID cells of WT

Please cite this article in press as: Xie et al., NAC1 regulates root ground tissue maturation by coordinating with the SCR/SHR–CYCD6;1 module in *Arabidopsis*, Molecular Plant (2023), https://doi.org/10.1016/j.molp.2023.02.006

roots at 5 dpg, was ectopically and highly expressed in the root ground tissue in *nac1-1* (Supplemental Figure 4A–4C), the ACDs of CEID cells appeared normal in the cortex/endodermal stem cell region of *nac1-1* and *nac1-2* mutants (Supplemental Figure 3A and 3B). We then examined whether NAC1 regulates root ground tissue maturation (middle cortex formation). Compared with the WT at 7 dpg, the *nac1-1, nac1-2, and nac1-1/nac1-2* F1 generation mutants exhibited a higher frequency of root middle cortex formation, and excessive periclinal cell divisions were observed in the endodermis of each mutant plant that exhibited a root middle cortex (Figure 1A–1D). However, the proportion of plants with a root middle cortex was greatly reduced in *mNAC1ox* lines (Supplemental Figure 5A–5C). Likewise, the increased frequency of root middle cortex formation and the excessive periclinal cell division phenotypes were completely or mostly restored to WT levels in *nac1-1/NAC1pro:NAC1* (Supplemental Figure 5D–5F), further confirming that these phenotypes were caused by the *NAC1* mutation. A time-course analysis showed that the root middle cortex formed earlier in the *nac1-1* mutants than in the WT (Figure 1E). These data suggest that NAC1 plays an important role in endodermal cell divisions during root middle cortex formation.

The NAC1–CYCD6;1 regulatory module controls root endodermal cell division to restrict excessive production of middle cortex cells

Given the important role of CYCD6;1 in endodermal cell divisions that form the root middle cortex (Koizumi et al., 2012a, 2012b), we examined the effect of *NAC1* on expression of the transcriptional reporter *CYCD6;1pro:GFP* (Sozzani et al., 2010). An increased proportion of roots with expanded *CYCD6;1pro:GFP* expression and enhanced GFP fluorescence in the endodermis, where CYCD6;1 promotes periclinal cell divisions to generate the root middle cortex, were detected in *nac1-1*. However, the *mNAC1ox-4* line showed a reduced proportion of plants with GFP expression and lower GFP fluorescence intensity (Figure 1F–1H).

To determine the genetic interactions between NAC1 and CYCD6;1, we crossed *nac1-1* with *cycd6;1*. In the *cycd6;1* mutant seedlings, the endodermis showed significantly fewer periclinal cell divisions at 7 dpg (Sozzani et al., 2010; Bertolotti et al., 2021). The excess periclinal cell divisions in the endodermis in the *nac1-1* mutant were largely rescued in the *nac1-1/cycd6;1* double mutant (Figure 1I–1K). Taken together, these results show that NAC1 plays an important role in root endodermal cell divisions to form the middle cortex in root tissue patterning by constraining spatiotemporal expression of *CYCD6;1*.

NAC1 directly inhibits the transcription of *CYCD6;1* by recruiting TPL

To confirm that NAC1 regulates the transcription level of *CYCD6;1*, we first examined the effect of NAC1 on *CYCD6;1* expression by qRT–PCR. Transcript levels of *CYCD6;1* were higher in *nac1-1* and lower in *mNAC1ox* compared with the WT (Figure 2A), consistent with the stronger GFP signals in *CYCD6;1pro:GFP/nac1-1* roots (Figure 1F–1H).

To examine whether NAC1 directly inhibits the transcription levels of *CYCD6;1*, we used a transient transcription *luciferase* (*LUC*) reporter assay in *Arabidopsis* protoplasts and found that LUC activity was decreased in protoplasts overexpressing *NAC1* with *CYCD6;1pro:LUC* as a reporter (Figure 2B). To determine whether NAC1 directly binds to the *CYCD6;1* promoter, we performed chromatin immunoprecipitation (ChIP)-qPCR with the *mNAC1ox-4* line and found that NAC1 interacted with the promoter of *CYCD6;1* (Figure 2C). Using an electrophoretic mobility shift assay (EMSA), we confirmed that NAC1 binds to two NAC recognition motifs (Olsen et al., 2005) within the promoter of *CYCD6;1* (P1 and P2) (Figure 2D). The interaction of NAC1 with the *CYCD6;1* promoter was also confirmed in yeast one-hybrid assays using the approximately −1537 to −555 bp fragment of the *CYCD6;1* promoter as bait (Figure 2E). Together, these results suggest that NAC1 directly inhibits expression of *CYCD6;1*.

NAC1 has been reported to activate target genes and contains a C-terminal activator domain (Xie et al., 2000). We noticed that the N-terminal region of NAC1 contains the sequence LVLIQVDLNKCEP, which contains two putative EAR motifs (LxL and DLNxxxP) (Ohta et al., 2001; Causier et al., 2012; Figure 3A). EAR motifs often interact with TPL family proteins or other co-repressors to inhibit expression of target genes (Causier et al., 2012). To determine whether NAC1 represses transcription of *CYCD6;1* by interacting with TPL, we performed a yeast two-hybrid assay and found that NAC1, but not NAC1mEAR with a mutated EAR motif (LVLIQVDLNKCEP to AVAIQVAHNKCEP), interacted with TPL (Figure 3B). Thus, NAC1 and TPL can interact, and this interaction depends on the EAR motif in NAC1. To further confirm the interaction between NAC1 and TPL *in planta*, we performed split-luciferase complementation assays and bimolecular fluorescence complementation (BiFC) assays. We detected luciferase signals when NAC1-cLUC and TPL-nLUC were co-expressed and observed YFP fluorescence upon co-expression of nYFP-NAC1 with cYFP-TPL, but not upon co-expression of the negative controls, indicating that TPL can interact with NAC1 in *Nicotiana benthamiana* (Figure 3C and 3D). In addition, TPL-YFP co-immunoprecipitated with NAC1-MYC from *Arabidopsis* mesophyll protoplasts (Figure 3E). Therefore, we infer that NAC1 can interact with TPL *in vitro* and *in vivo*.

Next, we examined whether the interaction with TPL is involved in NAC1 repression of *CYCD6;1*. Indeed, *CYCD6;1* was upregulated in the *tpl-9* and *tpl-10* mutants (Figure 3F and Supplemental Figure 6A; Li et al., 2019). We also observed reduced activity of the *CYCD6;1pro:LUC* reporter in *Arabidopsis* protoplasts that overexpressed *TPL* (Figure 3G). To better understand whether function of the NAC1–TPL complex underlies *CYCD6;1* induction, we expressed NAC1 and NAC1mEAR in WT and *tpl-9* mutant mesophyll protoplasts. We noted that NAC1, but not NAC1mEAR, could drastically repress *CYCD6;1* promoter activity in the WT background (Figure 3H). Furthermore, the NAC1 repression of *CYCD6;1* was completely disrupted in the *tpl-9* mutant background (Figure 3H). All of these results suggest that NAC1 directly inhibits *CYCD6;1* transcription by recruiting TPL.

TPL inhibits root endodermal cell division

Given the established role of CYCD6;1 in ACDs of CEID cells and the direct repression of *CYCD6;1* expression by NAC1

Please cite this article in press as: Xie et al., NAC1 regulates root ground tissue maturation by coordinating with the SCR/SHR–CYCD6;1 module in *Arabidopsis*, Molecular Plant (2023), https://doi.org/10.1016/j.molp.2023.02.006

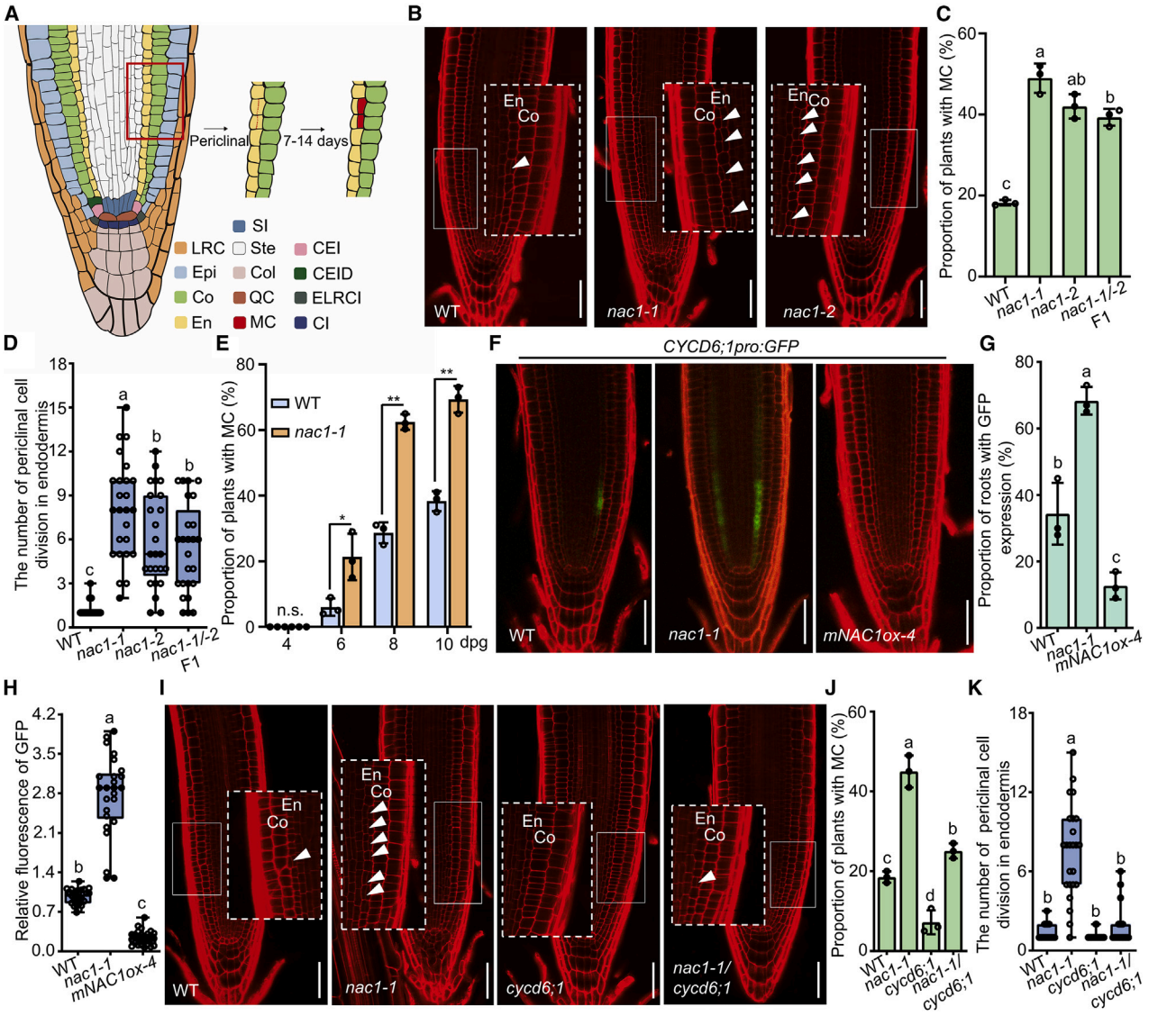

Figure 1. Knockdown of *NAC1* impairs middle cortex formation through upregulation of *CYCD6;1*.

(A) Organization of the *Arabidopsis* root meristem. Color-coded diagrams of a longitudinal section through the root meristem are shown. Away from the quiescent center (QC) toward the shoot is basal, whereas toward the root tip (apex) is apical. The cortex and endodermis are clonally related tissues derived from cortical endodermal initial (CEI) cells, which produce CEI daughter (CEID) cells. Asymmetric divisions of CEID cells produce the separate cortex and endodermis in a WT root. After about 7–14 days, asymmetric division of the endodermis produces the middle cortex. Thus, the mature primary root has three layers in the ground tissue. Ste, stele; En, endodermis; Co, cortex; Epi, epidermis; Col, columella; LRC, lateral root cap; MC, middle Co; CI, columella initial; SI, stele initial; ELRCI, Epi/LRC initial.

(B) Confocal images of ACDs in roots of 7-dpg WT, *nac1-1*, and *nac1-2* seedlings. The insets in **(B)** illustrate periclinal ACDs that generate the middle cortex layers. The periclinal ACDs are indicated with white arrowheads. Scale bars, 50 μm.

(C) Proportion of plants with middle cortex in the WT, *nac1-1*, and *nac1-2*.

(D) The number of periclinal cell divisions in the En of each plant exhibiting root middle cortex as shown in **(B)**.

(E) Time-course analysis of middle cortex formation in the WT and *nac1-1* mutants at the indicated time points (4, 6, 8, and 10 dpg).

(F) *CYCD6;1pro:GFP* fusion expression pattern in the WT, *nac1-1*, and *mNAC1ox-4*. The seedlings were photographed at 7 dpg. Scale bar, 50 μm.

(G) Proportion of roots with GFP expression as shown in **(F)**.

(H) Quantification of GFP fluorescence as shown in **(F)**. The GFP signal intensity of each genotype was normalized relative to that of the WT.

(I) Confocal images of ACDs in roots of 7-dpg WT, *nac1-1*, *cycd6;1*, and *nac1-1/cycd6;1* seedlings. The insets illustrate periclinal ACDs that generate the middle cortex layers. The periclinal ACDs are indicated with white arrowheads. Scale bars, 50 μm.

(J) Proportion of plants with middle cortex in the WT, *nac1-1*, *cycd6;1*, and *nac1-1/cycd6;1*.

(K) The number of periclinal cell divisions in the En of each plant exhibiting root middle cortex as shown in **(H)**.

In **(D)**, **(H)**, and **(K)**, individual values (black dots) are shown. In **(C)**, **(E)**, **(G)**, and **(J)**, data represent mean ± SE of three biological replicates. In **(C)** and **(J)**, n > 30 for each biological replicate; in **(G)**, n = 35 for each biological replicate; in **(D)**, **(H)**, and **(K)**, n = 25. Different lowercase letters above bars indicate a significant difference (one-way ANOVA, Tukey's multiple comparison test, $P < 0.05$). In **(E)**, n > 35 for each biological replicate; data represent mean ± SE of three biological replicates (**$P < 0.01$, *$P < 0.05$, Student's *t*-test).

Please cite this article in press as: Xie et al., NAC1 regulates root ground tissue maturation by coordinating with the SCR/SHR–CYCD6;1 module in *Arabidopsis*, Molecular Plant (2023), https://doi.org/10.1016/j.molp.2023.02.006

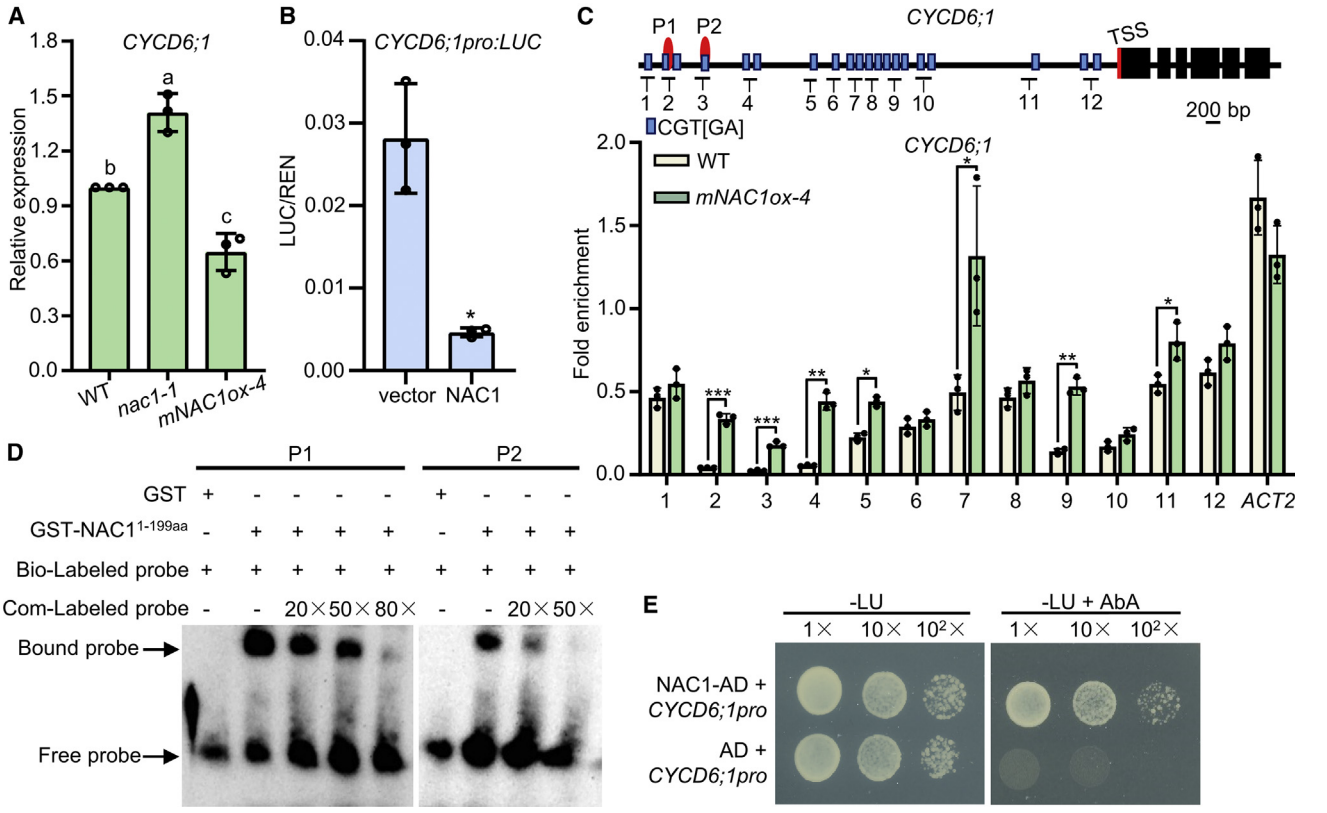

Figure 2. NAC1 directly binds to the *CYCD6;1* promoter.

(A) qRT–PCR analysis showing the relative expression levels of *CYCD6;1* in the WT, *nac1-1*, and *mNAC1ox-4*. Total RNA was extracted from primary roots of 7-dpg seedlings. The expression level in the WT was set to "1." Three biological replicates with three technical replicates for each biological replicate were performed with similar results. Data represent mean ± SE of three biological replicates. Different letters above bars indicate a significant difference (one-way ANOVA, Tukey's multiple comparison test, $P < 0.05$).

(B) NAC1 *trans*-represses the *CYCD6;1* promoter in *Arabidopsis* leaf protoplasts. The empty vector *pBI221* was used as a negative control. Three biological replicates with three technical replicates for each biological replicate were performed with similar results. Data represent mean ± SE of three biological replicates. An asterisk indicates a significant difference ($^*P < 0.05$) from the negative control.

(C) Schematic of *CYCD6;1* and the PCR amplicons (1–12) used for ChIP-qPCR. TSS, transcription start site. ChIP-qPCR results show the enrichment of NAC1 on the chromatin of *CYCD6;1*. Sonicated chromatin from 7-dpg seedlings (*35S::MYC-mNAC1*) was precipitated with anti-MYC antibodies. The precipitated DNA was used as a template for qPCR analysis with primers targeting different regions of *CYCD6;1* as shown in **(C)**. Three biological replicates with three technical replicates for each biological replicate were performed with similar results. Data represent mean ± SE of three biological replicates. $^{***}P < 0.001$, $^{**}P < 0.01$, $^*P < 0.05$, Student's *t*-test.

(D) EMSA showing that NAC1 (1–199 amino acids) binds the putative motif in the *CYCD6;1* promoter. The biotin-labeled probes (P1 and P2) are indicated in **(C)**. Unlabeled probes were used in the competition assay.

(E) Yeast one-hybrid binding assay involving NAC1 and the *CYCD6;1* promoter. The yeast transformants were dropped onto SD−Leu−Ura (−Leu, −Ura) medium. The yeast transformants were dropped onto SD−Leu−Ura (−Leu, −Ura) medium with 160 ng/ml Aureobasidin A (AbA). The *CYCD6;1* promoter spans from −1573 to −555 bp.

through TPL recruitment, we next examined the role of TPL in the ACDs of CEID cells. We examined three *tpl* mutants (*tpl-1*, *tpl-9*, and *tpl-10*) (Supplemental Figure 6A) and found that these three mutant alleles did not significantly alter the ACDs of CEID cells (Supplemental Figure 6B and 6C). The role of TPL in producing root middle cortex cells was also examined. Compared with the WT, more *tpl-1*, *tpl-9*, and *tpl-10* mutants exhibited a root middle cortex, and each mutant plant that exhibited a root middle cortex also showed excessive periclinal cell divisions in the endodermis (Figure 4A–4C). Similar to the *nac1-1* mutant, *tpl-1* plants also showed altered timing of root middle cortex formation compared with the WT (Figure 4D). Compared with WT roots at 7 dpg, an increased proportion of *tpl-9* roots showed expanded *CYCD6;1pro:GFP* expression and enhanced GFP fluorescence in the endodermis (Figure 4E–4G). Collectively, our data show that NAC1 recruits TPL to inhibit *CYCD6;1* expression and excessive periclinal cell divisions of the endodermis during root ground tissue maturation.

NAC1 interacts directly with SCR and SHR

The two GRAS transcription factors SCR and SHR have been reported to play key roles in middle cortex formation during root ground tissue maturation (Paquette and Benfey, 2005). We next investigated whether NAC1 physically interacts with SCR or SHR. Yeast two-hybrid assays showed that NAC1 interacts with SCR and SHR *in vitro* (Figure 5A), and

Please cite this article in press as: Xie et al., NAC1 regulates root ground tissue maturation by coordinating with the SCR/SHR–CYCD6;1 module in *Arabidopsis*, Molecular Plant (2023), https://doi.org/10.1016/j.molp.2023.02.006

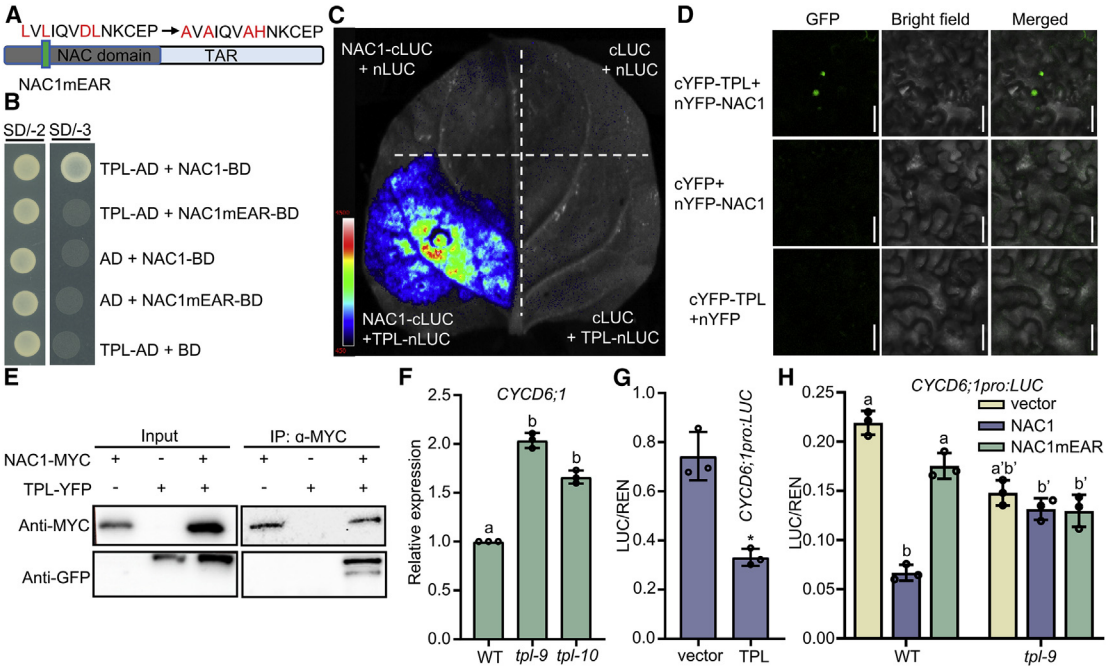

Figure 3. NAC1 recruits TPL to directly repress *CYCD6;1*.

(A) NAC1mEAR is mutated NAC1 in which the core LVLIQVDLNKCEP residues of the EAR motif were changed to AVAIQVAHNKCEP. The mutated amino acids of the EAR motif are indicated in red.

(B) Interaction of NAC1 or NAC1mEAR with TPL in a yeast two-hybrid assay. Yeast cells were grown on SD/−Trp/−Leu (SD/−2) and SD/−Trp/−Leu/−His (SD/−3) media. Yeast cells co-transformed with *pGBKT7-NAC1* or *pGBKT7-NAC1mEAR* derivatives (bait) and *pGADT7-TPL* (prey) were dropped onto SD/−2 and SD/−3 media to assess interactions with TPL.

(C) A split-luciferase complementation assay shows the interaction of NAC1-cLUC and TPL-nLUC in *N. benthamiana* leaves; nLUC with NAC1-cLUC, cLUC with TPL-nLUC, and cLUC with nLUC were used as negative controls.

(D) BiFC assay showing that NAC1 interacts with TPL under white-light conditions. *N. benthamiana* was co-transformed with nYFP-NAC1 and cYFP-TPL, nYFP and cYFP-TPL, and nYFP-NAC1 and cYFP. Merge, overlay of the YFP and bright-field images. Scale bar, 50 μm.

(E) NAC1-MYC was co-expressed with TPL-YFP in *Arabidopsis* mesophyll protoplasts. Protein extracts (input) were immunoprecipitated with anti-MYC antibody. Immunoblots were developed with anti-GFP antibody to detect TPL-YFP and with anti-MYC to detect NAC1-MYC.

(F) qRT–PCR analysis showing the relative expression levels of *CYCD6;1* in the WT, *tpl-9*, and *tpl-10*. Total RNA was extracted from primary roots of 7-dpg seedlings. The expression level in the WT was set to "1." Three biological replicates with three technical replicates for each biological replicate were performed with similar results. Data represent mean ± SE of three biological replicates. Different letters above bars indicate a significant difference (one-way ANOVA, Tukey's multiple comparison test, $P < 0.05$).

(G) TPL *trans*-represses the *CYCD6;1* promoter in *Arabidopsis* leaf protoplasts. The empty vector *pBI221* was used as a negative control. Three biological replicates with three technical replicates for each biological replicate were performed with similar results. Data represent mean ± SE of three biological replicates (Student's *t*-test, $^*P < 0.05$).

(H) Relative activity of the *CYCD6;1pro:LUC* reporter in *Arabidopsis* WT- and *tpl-9*-background protoplasts co-transformed with the indicated effector constructs. Three biological replicates with three technical replicates for each biological replicate were performed with similar results. Data represent mean ± SE of three biological replicates. Different letters above bars indicate a significant difference. In the WT- or *tpl-9* background, different lower-case letters indicate significant differences by one-way ANOVA followed by Tukey's multiple comparison test ($P < 0.05$).

co-immunoprecipitation assays in protoplast cells showed that NAC1 and SCR or SHR form a complex *in vivo* (Figure 5B). The interaction of NAC1 with SCR and SHR was also confirmed in *N. benthamiana* leaves by split-luciferase complementation assays and BiFC assays (Figure 5C and 5D). Interestingly, domain mapping analysis indicated that the central domain (CD) (Cui et al., 2007) of SCR was involved in the interaction between NAC1 and SCR (Figure 5E and 5F).

NAC1 acts in the SCR/SHR pathway to regulate root endodermal cell divisions

Previous studies have shown that the root middle cortex fails to form in the *shr-2* mutant, whereas periclinal cell divisions in the single layer of root ground tissue appear at early time points and show a higher frequency in the *scr-5* mutant compared with the WT control. These results suggest that SHR is required for formation of the root middle cortex, whereas SCR plays a negative role in this process (Paquette and Benfey, 2005). To gain insight into the genetic relationship of NAC1 with SCR and SHR, we generated the *nac1-1/scr-2* and *nac1-1/shr-2* double mutants and examined their root middle cortex formation phenotypes. Similar to the *shr-2* mutant, the *nac1-1/shr-2* double mutant failed to undergo root middle cortex formation (Figure 6A–6C). By contrast, root middle cortex formation was markedly increased in the *nac1-1/scr-2* double mutant, similar to that observed in *scr-2* (Figure 6A–6C). Taken together, these results indicate that *SHR* and *SCR* are genetically epistatic to *NAC1* and required for repression of root middle cortex formation by NAC1.

Please cite this article in press as: Xie et al., NAC1 regulates root ground tissue maturation by coordinating with the SCR/SHR–CYCD6;1 module in *Arabidopsis*, Molecular Plant (2023), https://doi.org/10.1016/j.molp.2023.02.006

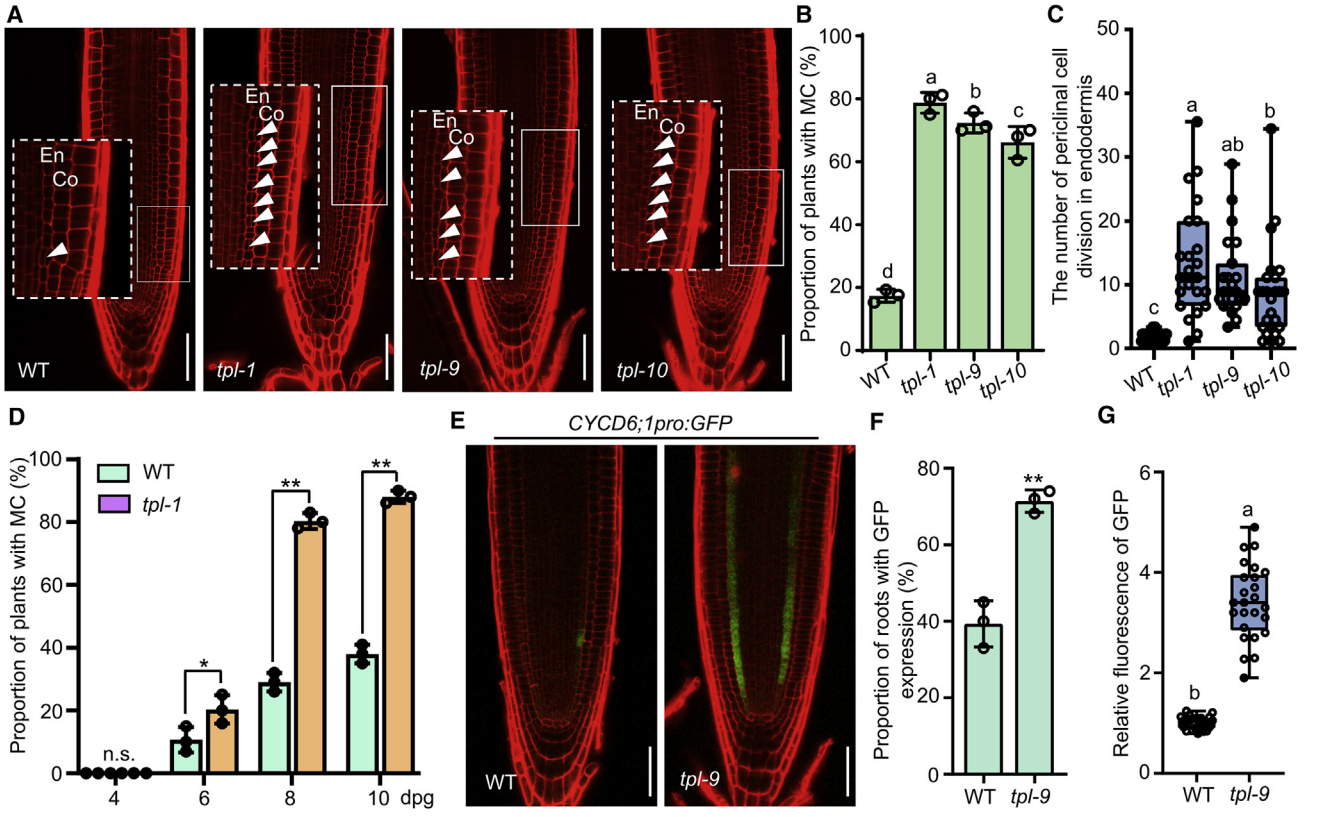

Figure 4. TPL negatively regulates the endodermal cell division.

(A) Confocal images of ACDs in roots of 7-dpg WT, *tpl-1*, *tpl-9*, and *tpl-10* seedlings. The insets illustrate periclinal ACDs that generate the En and middle cortex layers. The periclinal ACDs are indicated with white arrowheads. Scale bars, 50 μm.

(B) Proportion of plants with middle cortex in WT, *tpl-1*, *tpl-9*, and *tpl-10*. The frequency of periclinal ACDs for middle cortex formation was analyzed at 7 dpg. n > 35 for each biological replicate; data represent mean ± SE of three biological replicates. Different letters above bars indicate a significant difference (one-way ANOVA, Tukey's multiple comparison test, $P < 0.05$).

(C) The numbers of periclinal cell divisions in the En of each plant that exhibited root middle cortex as shown in **(A)**; data represent mean ± SD. Individual values (black dots) are shown (n > 22). Different lowercase letters indicate significant differences by one-way ANOVA followed by Tukey's multiple comparison test ($P < 0.05$).

(D) Time-course analysis of middle cortex formation in WT and *tpl-1* mutants at the indicated time points (4, 6, 8, and 10 dpg). n > 35 for each biological replicate; data represent mean ± SE of three biological replicates. $^{**}P < 0.01$, $^{*}P < 0.05$, Student's *t*-test.

(E) Confocal images of *CYCD6;1pro:GFP* fusion expression in roots of 7-dpg WT and *tpl-9*. Scale bar, 50 μm.

(F) Proportion of roots with GFP expression as shown in **(E)**. n = 30 for each biological replicate; data represent mean ± SE of three biological replicates. $^{**}P < 0.01$, Student's *t*-test.

(G) Quantification of GFP fluorescence as shown in **(E)**. GFP signal intensity of each genotype was normalized relative to that of the WT. Data represent mean ± SD. Individual values (black dots) are shown (n = 25). Different lowercase letters indicate significant differences by one-way ANOVA followed by Tukey's multiple comparison test ($P < 0.05$).

We also examined the effects of NAC1, SHR, and SCR on local transcription of *CYCD6;1* (*CYCD6;1pro:GFP*) and found that GFP expression was strongly upregulated in the endodermis of *nac1-1*, *scr-2*, and *nac1-1/scr-2* compared with that of the WT (Figure 6D–6F). By contrast, almost no expression of *CYCD6;1* was observed in *shr-2* and *nac1-1/shr-2* mutant roots (Figure 6D–6F). These results were consistent with the periclinal cell division phenotypes of the mutants (Figure 6A–6C).

SCR is required for restriction ofroot endodermal cell divisions by NAC1

To further dissect the effect of SCR on the restriction of root middle cortex cell production by NAC1, we crossed *mNAC1ox-4* with *35S::SCR-YFP*. Although *35S::SCR-YFP* had a middle cortex phenotype similar to that of the WT, it rescued the short-root phenotype and the increased root middle cortex phenotype of *scr-2* (Supplemental Figure 7A–7E). *35S::SCR-YFP/mNAC1ox-4* showed no difference in the extent of periclinal cell division but a reduced proportion of plants with a root middle cortex compared with *mNAC1ox-4* (Figure 7A–7C). However, the proportion of plants with root middle cortex formation and the extent of periclinal cell divisions in the single layer of root ground tissue in *scr-2/mNAC1ox-4* were similar to those in *scr-2* but much higher than those in *mNAC1ox-4* (Figure 7E–7G). These results clearly indicated that SCR is required for restriction of excessive periclinal divisions in the endodermis by NAC1 during root middle cortex formation.

Please cite this article in press as: Xie et al., NAC1 regulates root ground tissue maturation by coordinating with the SCR/SHR–CYCD6;1 module in *Arabidopsis*, Molecular Plant (2023), https://doi.org/10.1016/j.molp.2023.02.006

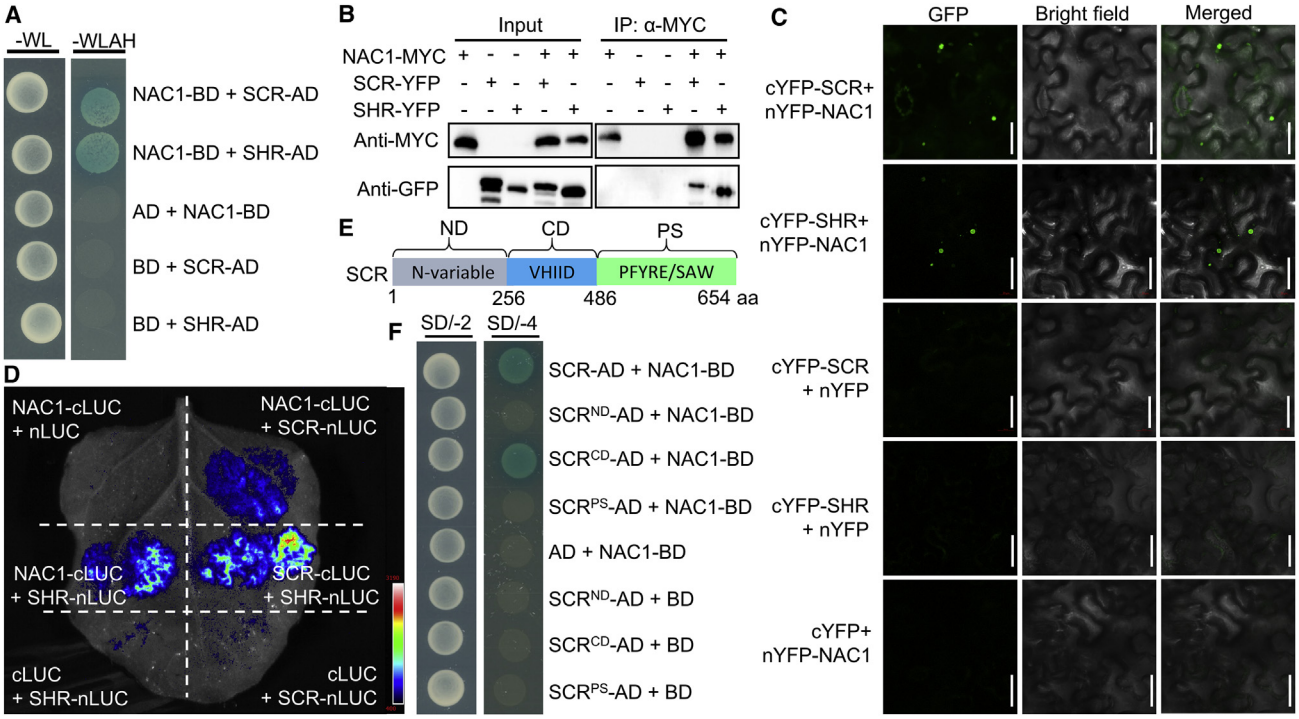

Figure 5. NAC1 interacts with SCR and SHR in the nucleus.

(A) Interaction of NAC1 and SCR or SHR in a yeast two-hybrid assay. Yeast cells were grown on SD/−Trp/−Leu (−WL) and SD/−Trp/−Leu/−His/−Ade (−WLAH) media. Yeast cells co-transformed with *pGADT7-SCR* or *pGADT7-SHR* derivatives (bait) and *pGBKT7-NAC1* (prey) were dropped onto −WL and −WLAH media with 5 mM 3-Amino-1,2,4-triazole, AbA, and 5-BroMo-4-chloro-3-indolyl-α-D-galactopyranoside to assess interactions with NAC1.

(B) CoIP of NAC1 with SCR and SHR. NAC1-MYC was co-expressed with SCR-YFP or SHR-YFP in *Arabidopsis* mesophyll protoplasts. Protein extracts (input) were immunoprecipitated with anti-MYC antibody. Immunoblots were developed with anti-GFP antibody to detect SCR-YFP or SHR-YFP and with anti-MYC to detect NAC1-MYC.

(C) BiFC assay showing that NAC1 interacts with SCR and SHR under white-light conditions. *N. benthamiana* was co-transformed with nYFP-NAC1 and cYFP, nYFP, and cYFP-SCR or cYFP-SHR. Merge, overlay of the YFP and bright-field images. Scale bar, 50 μm.

(D) A split-luciferase complementation assay shows the interaction of NAC1-cLUC with SCR-nLUC and SHR-nLUC and SCR-cLUC with SHR-nLUC in *N. benthamiana* leaves; nLUC with NAC1-cLUC and cLUC with SCR-nLUC and SHR-nLUC were used as the negative controls.

(E) Schematic of the protein domains of SCR.

(F) Interaction of NAC1 and truncated SCR in a yeast two-hybrid assay. Yeast cells were grown on SD/−2 and SD/−Trp/−Leu/−His/−Ade media. Yeast cells co-transformed with *pGBKT7-NAC1* derivative (bait) and *pGADT7-SCR* or truncated SCR (prey) were dropped onto SD/−2 and SD/−Trp/−Leu/−His/−Ade media to assess interactions with SCR.

Because CYCD6;1 is important for periclinal division of the endodermis, we investigated whether NAC1 regulates *CYCD6;1* expression together with SCR. qRT–PCR revealed that *CYCD6;1* expression was dramatically reduced in *35S::SCR-YFP/mNAC1ox-4* seedlings compared with *35S::SCR-YFP* or *mNAC1ox-4* seedlings (Figure 7D), whereas *CYCD6;1* expression was markedly increased in *scr-2/mNAC1ox-4* seedlings compared with *mNAC1ox-4* seedlings (Figure 7H). Thus, SCR is required for repression of *CYCD6;1* expression by NAC1.

Next, we examined the effect of SCR and NAC1 on transient expression of *CYCD6;1pro:LUC* in *Arabidopsis* leaf protoplasts. When *SCR* or *TPL* was co-expressed with *NAC1*, LUC activity was reduced compared with either gene alone (Figure 7I). When *TPL* was simultaneously co-expressed with *SCR* and *NAC1*, LUC activity was further inhibited (Figure 7I). These results support the notion that NAC1 recruits the co-repressor TPL together with SCR to control expression of the *CYCD6;1* gene. Next, we performed ChIP-qPCR assays to examine whether SCR is required for binding of NAC1 to the *CYCD6;1* promoter regions. We quantified binding of NAC1 to the *CYCD6;1* promoter in *mNAC1ox-4*, *35S::SCR-YFP/mNAC1ox-4*, and *scr-2/mNAC1ox-4* seedlings. Bound *CYCD6;1 promoter fragments were highly enriched in 35S::SCR-YFP/mNAC1ox-4 seedlings but not in scr-2/mNAC1ox-4 seedlings compared with mNAC1ox-4* (Figure 7J), indicating that SCR is required for association between the *CYCD6;1* promoter and NAC1. Taken together, our data indicate that NAC1 directly regulates *CYCD6;1* transcription and periclinal cell division of the endodermis during root middle cortex formation by interacting with SCR.

SHR and NAC1 antagonize each other to regulate periclinal cell division of the endodermis during root middle cortex formation

Because initiation of root middle cortex formation appears to require SHR function, we evaluated the relationship between NAC1 and SHR. We generated *mNAC1ox-4/35S::SHR-GFP* double overexpression lines for phenotype analysis and found that overexpression of *SHR* (*35S::SHR-GFP*) induced formation of

Please cite this article in press as: Xie et al., NAC1 regulates root ground tissue maturation by coordinating with the SCR/SHR–CYCD6;1 module in *Arabidopsis*, Molecular Plant (2023), https://doi.org/10.1016/j.molp.2023.02.006

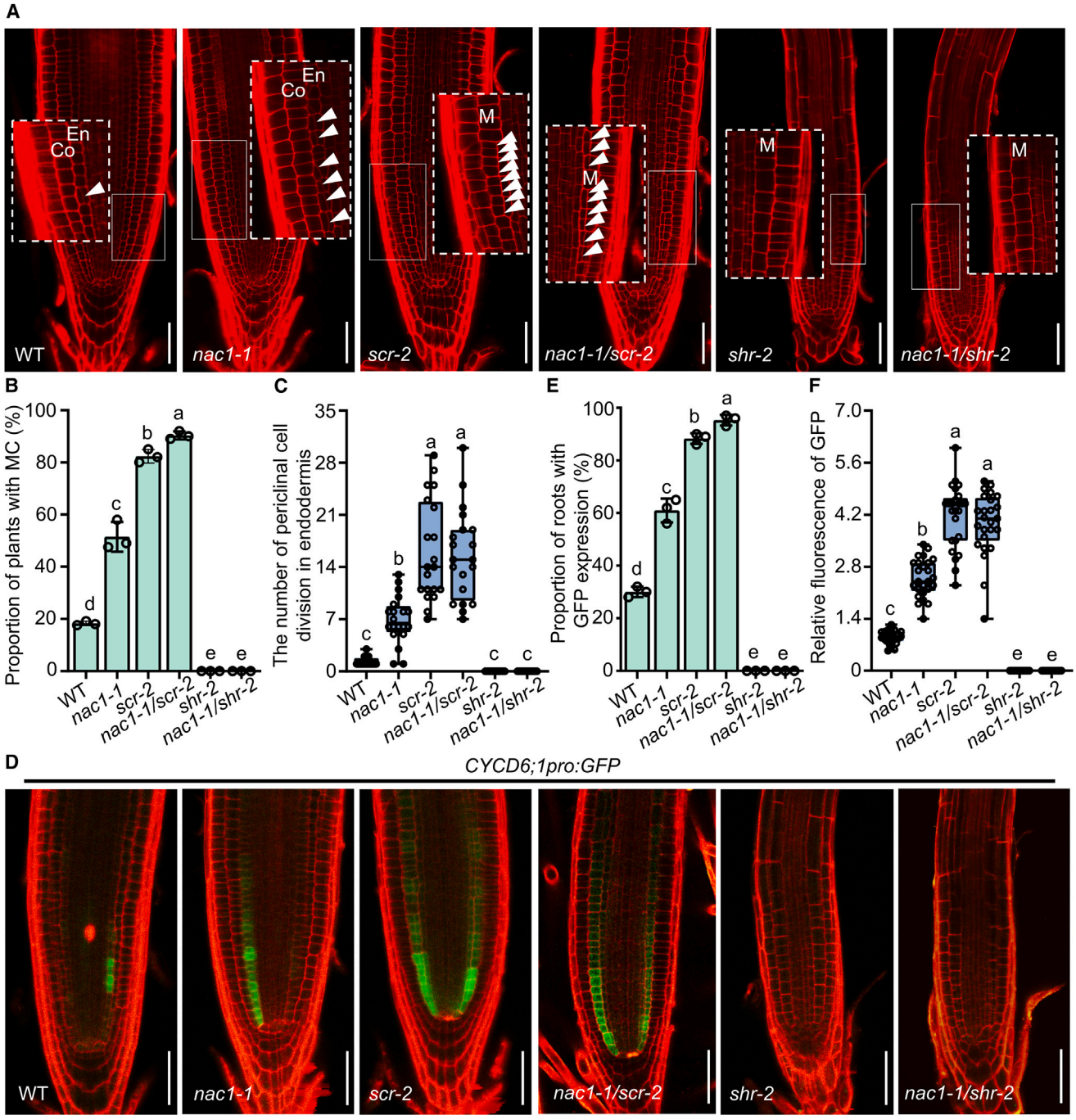

Figure 6. NAC1 functions together with the SCR/SHR pathway in middle cortex formation.

(A) Confocal images of ACDs in roots of 7-dpg WT, *nac1-1*, *scr-2*, *nac1-1/scr-2*, *shr-2*, and *nac1-1/shr-2* seedlings. The insets illustrate periclinal ACDs that generate the middle cortex layers. M, mutant cell layer. The periclinal ACDs are indicated with white arrowheads. Scale bars, 50 μm.

(B) Proportion of plants with middle cortex in the WT, *nac1-1*, *scr-2, nac1-1/scr-2, shr-2,* and *nac1-1/shr-2*. n > 35 for each biological replicate; data represent mean ± SE of three biological replicates. Different letters above bars indicate a significant difference (one-way ANOVA, Tukey's multiple comparison test, $P < 0.05$).

(C) The numbers of periclinal cell divisions in the En of each plant that exhibited root middle cortex as shown in **(A)**; data represent mean ± SD. Individual values (black dots) are shown (n = 20). Different lowercase letters indicate significant differences by one-way ANOVA followed by Tukey's multiple comparison test ($P < 0.05$).

(D) Confocal images of *CYCD6;1pro:GFP* fusion expression in roots of 7-dpg WT, *nac1-1*, *scr-2*, *nac1-1/scr-2*, *shr-2*, and *nac1-1/shr-2*. Scale bar, 50 μm.

(legend continued on next page)

Please cite this article in press as: Xie et al., NAC1 regulates root ground tissue maturation by coordinating with the SCR/SHR–CYCD6;1 module in *Arabidopsis*, Molecular Plant (2023), https://doi.org/10.1016/j.molp.2023.02.006

supernumerary endodermal cell layers (Helariutta et al., 2000; Yu et al., 2017), which were partially suppressed in *mNAC1ox-4/35S::SHR-GFP* (Supplemental Figure 8A and 8B). In addition, supernumerary endodermal cell layers were still observed in *nac1-1/35S::SHR-GFP* (Supplemental Figure 9A and 9B). Similar to the *shr-2* mutant, *shr-2/mNAC1ox-4* plants also failed to form a root middle cortex (Supplemental Figure 8D and 8E).

CYCD6;1 is a direct transcriptional target of SHR and NAC1, and we next investigated the relationship between NAC1 and SHR in regulation of *CYCD6;1* transcription. qRT–PCR analysis revealed that the repression and enhancement of *CYCD6;1* expression by overexpression of *NAC1* and *SHR*, respectively, were largely rescued in the *mNAC1ox-4/35S::SHR-YFP* line (Supplemental Figure 8C). The *shr-2* mutant and the *shr-2/mNAC1ox-4* line showed a very similar expression level of *CYCD6;1* (Supplemental Figure 8F). Furthermore, qRT–PCR assays indicated that *CYCD6;1* transcript levels were higher in *nac1-1/35S::SHR-GFP* than in *35S::SHR-GFP* (Supplemental Figure 9C). Together, these results indicate that NAC1 and SHR function antagonistically in the regulation of *CYCD6;1* expression.

We then analyzed whether SHR affected the transcription activity of NAC1 on the *CYCD6;1* promoter using transient expression assays in WT and *shr-2* protoplasts (Supplemental Figure 8G). Expression of *CYCD6;1pro:LUC* was significantly lower in *shr-2* mutant protoplasts when co-expressed with NAC1 than in the WT background (Supplemental Figure 8G). Furthermore, ChIP-qPCR assays showed that the higher enrichments of NAC1-bound *CYCD6;1* promoter regions in *mNAC1ox-4* were markedly reduced in *mNAC1ox-4/35S::SHR-GFP* (Supplemental Figure 8H). These results indicate that SHR inhibits recruitment of NAC1 to the *CYCD6;1* promoter. To examine whether NAC1 affects the binding of SHR to the *CYCD6;1* promoter region, we performed ChIP-qPCR assays using *35S::SHR-GFP* and *mNAC1ox-4/35S::SHR-GFP* transgenic plants. The results showed that the higher enrichment of fragment B within the *CYCD6;1* promoter in the *35S::SHR-GFP* line was completely abolished in the *mNAC1ox-4/35S::SHR-GFP* line (Supplemental Figure 9D). Interestingly, enriched fragment B (approximately −1367 to −1164 bp) bound by SHR in the *CYCD6;1* promoter is adjacent to enriched fragment 11 (approximately −1536 to −1349 bp) bound by NAC1 (Figure 2C), suggesting that NAC1 and SHR may compete for the same region on the *CYCD6;1* promoter. Taken together, these data indicate that NAC1 and SHR antagonize each other to regulate spatiotemporal expression of *CYCD6;1* during root middle cortex formation.

DISCUSSION

In this study, we uncovered a crucial role for NAC1 in root ground tissue patterning through direct transcriptional inhibition of *CYCD6;1*, a process that is mediated by interaction with the transcriptional co-repressor TPL (Figure 7K). This study, together with previous reports, reveals that NAC family proteins play extensive and critical roles in shoot and root stem cell maintenance.

The expression of *CYCD6;1* coincides with the onset of specific ACDs of the CEI and CEID cells and with ACD of endodermal cells to form the middle cortex, thereby patterning the root ground tissue (Sozzani et al., 2010). Although the strict spatiotemporal expression pattern of *CYCD6;1pro:GFP* was ectopically expressed in the root endodermis in *nac1-1* and *tpl-9*, the formative divisions of CEID cells were not affected in *nac1* and *tpl* mutant roots. It appears that TPL and NAC1 may not be involved in the formative divisions of the CEID cells or that TPL and NAC1 may share redundant roles with other involved factors. A previous study showed that the cell differentiation factor RETINOBLASTOMA-RELATED could interact with the N-terminal conserved LxCxE motif of SCR to inhibit *CYCD6;1* expression in the root (Cruz-Ramírez et al., 2012). Furthermore, our study showed that NAC1 could bind to the CD of SCR. Thus, it will be interesting in future studies to determine whether NAC1 interacts with RETINOBLASTOMA-RELATED to control the ACDs of CEID cells in the root.

SCR has been reported to restrict the timing of initiation of periclinal cell divisions in the endodermis and the first divisions of endodermal cells to form the middle cortex located next to the phloem poles (Paquette and Benfey, 2005; Koizumi et al., 2012a, 2012b). Here, we found that *nac1* mutants show dramatically impaired root middle cortex formation, revealing a previously unidentified function of NAC1 in regulating the endodermal cell divisions that form the middle cortex. Intriguingly, NAC1 negatively regulates *CYCD6;1* expression in root ground tissue, and eliminating *CYCD6;1* function in the *nac1* mutant restored the ground tissue patterning defects. These data indicate that NAC1 is required for spatial restriction of periclinal cell divisions in the endodermis.

From embryogenesis to the early stages of post-embryonic development, *scr* mutants have a single ground tissue layer with mixed traits of the endodermis and cortex, whereas *shr* mutants have a single cell layer with only cortex attributes (Benfey et al., 1993; Scheres et al., 1995; Di Laurenzio et al., 1996; Cruz-Ramírez et al., 2012). Subsequently, sporadic middle cortex layers are precociously produced in the *scr* root, but these layers fail to form in the *shr* mutant (Paquette and Benfey, 2005; Cui and Benfey, 2009a, 2009b; Heo et al., 2011; Koizumi et al., 2012a). In the present study, the *nac1/scr* double mutant exhibited similar periclinal cell divisions of the single layer of root ground tissue compared with the *scr* single mutant, and both the *nac1/shr* double mutant and the *shr* single mutant failed to form a root middle cortex. This result indicated that NAC1 restricts excessive periclinal cell divisions of the endodermis during root middle cortex formation, a process that is dependent on an SCR- and SHR-mediated pathway

(E) Proportion of roots with GFP expression as shown in **(D)**. n = 30 for each biological replicate; data represent mean ± SE of three biological replicates. Different letters above bars indicate a significant difference (one-way ANOVA, Tukey's multiple comparison test, $P < 0.05$).
(F) Quantification of GFP fluorescence as shown in **(D)**. GFP signal intensity of each genotype was normalized relative to that of the WT. Data represent mean ± SD. Individual values (black dots) are shown (n = 25). Different lowercase letters indicate significant differences by one-way ANOVA followed by Tukey's multiple comparison test ($P < 0.05$).

Please cite this article in press as: Xie et al., NAC1 regulates root ground tissue maturation by coordinating with the SCR/SHR–CYCD6;1 module in *Arabidopsis*, Molecular Plant (2023), https://doi.org/10.1016/j.molp.2023.02.006

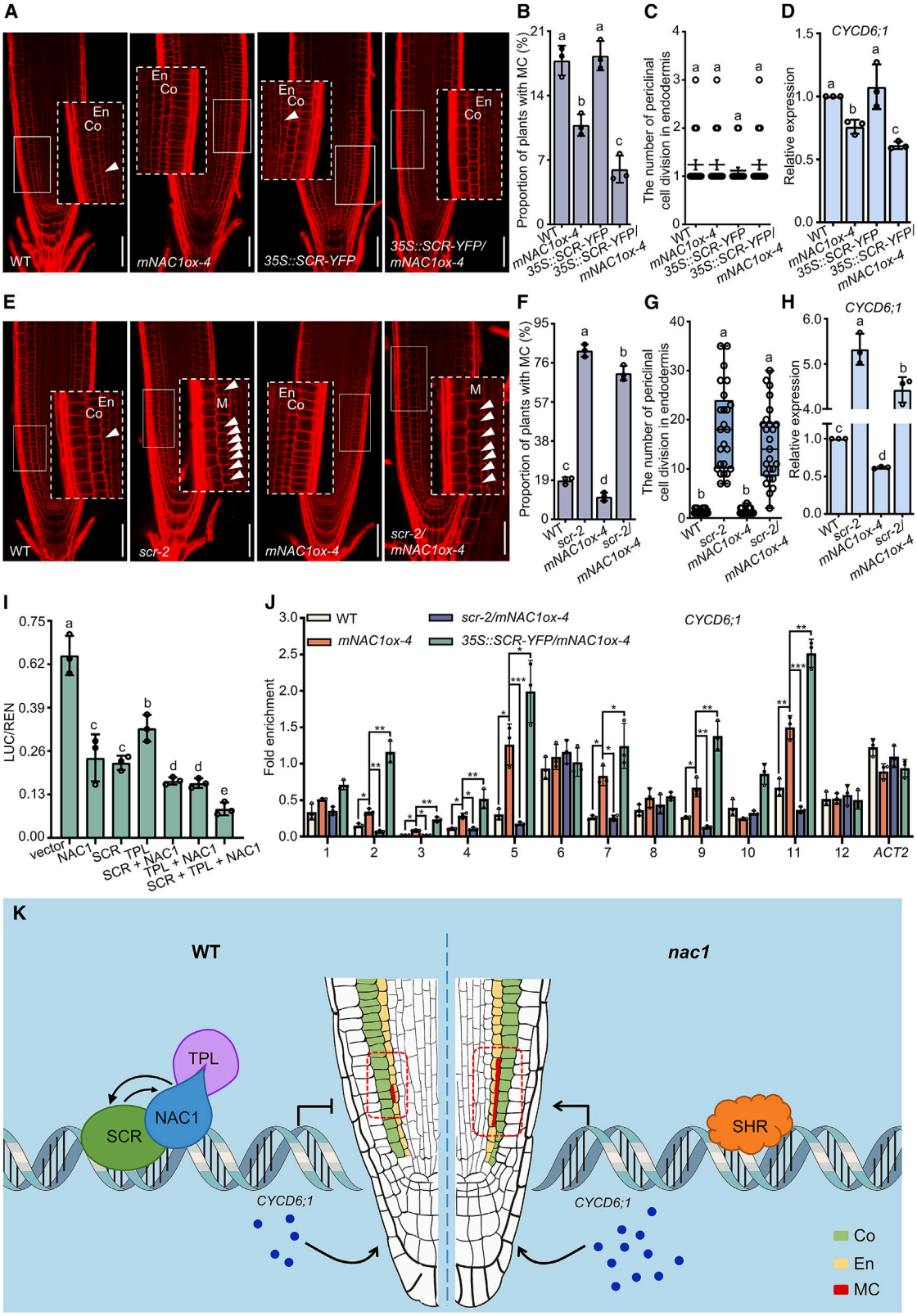

Figure 7. SCR is involved in NAC1 repression of middle cortex formation.

(A) Confocal images of ACDs in roots of 7-dpg WT, *mNAC1ox-4*, *35S::SCR-YFP* and *35S::SCR-YFP/mNAC1ox-4* seedlings. The insets illustrate periclinal ACDs that generate the En and middle cortex layers. The periclinal ACDs are indicated with white arrowheads. Scale bars, 50 μm.

(legend continued on next page)

Please cite this article in press as: Xie et al., NAC1 regulates root ground tissue maturation by coordinating with the SCR/SHR–CYCD6;1 module in *Arabidopsis*, Molecular Plant (2023), https://doi.org/10.1016/j.molp.2023.02.006

(Figure 7K). Although SCR has been reported to negatively regulate root middle cortex formation, little is known about how SCR represses *CYCD6;1* expression. Our data imply a key role for NAC1 in this mechanism. It is reasonable to speculate that NAC1 recruits the co-repressor TPL to form a complex with SCR and thus directly represses the expression of *CYCD6;1*. This interpretation would explain the similar root middle cortex phenotypes of *nac1* and *scr*. Alternatively, NAC1–TPL and SCR might function together to repress SHR activity and thus inhibit *CYCD6;1* expression. Interestingly, MED31 has also been shown to bind to the CD of SCR, similar to NAC1, but activate the SHR/SCR transcriptional targets (Zhang et al., 2018). Therefore, we predict that NAC1 abundance is high enough to compete with MED31 for binding to SCR during root middle cortex formation. The relationship between NAC1 and MED31 binding to SCR will need to be elucidated in future studies. Taken together, the present findings suggest that, on one hand, NAC1–TPL restricts excessive periclinal division of the endodermis by repressing *CYCD6;1* expression during root middle cortex formation in an SCR-dependent manner (Figure 7K). On the other hand, NAC1 and SHR antagonize each other to bind to the *CYCD6;1* promoter, suggesting an antagonistic role of NAC1 and SHR in root middle cortex formation (Figure 7K).

GA signaling has been reported to prevent initiation of middle cortex formation, and GA acts synergistically or additively with the SHR/SCR module in control of middle cortex formation (Paquette and Benfey, 2005; Cui and Benfey, 2009a; Heo et al., 2011; Gong et al., 2016; Lee et al., 2016). SCL3, a member of the GRAS family of transcription factors, plays a key role in GA/DELLA and SHR/SCR pathways to modulate the timing and extent of middle cortex formation (Heo et al., 2011; Gong et al., 2016; Lee et al., 2016). It will be very interesting in future studies to determine whether NAC1 is involved in GA-mediated middle cortex formation through crosslinking with SCL3.

NAC1 is necessary and sufficient for auxin signal transduction downstream of TIR1 during lateral root development (Xie et al., 2000). Auxin also promotes *CYCD6;1* transcription during two ACDs of the CEI cells and CEID cells to produce the endodermis and cortex (Cruz-Ramírez et al., 2012). In addition, jasmonic acid and auxin signaling synergize to induce *CYCD6;1* during root regeneration (Zhou et al., 2019). Wounding is an early trigger of plant regeneration, and wounding-induced NAC1 acts independently of auxin during *de novo* root organogenesis from leaf explants (Chen et al., 2016). We propose that NAC1 provides a complex mixture of signals that have multiple roles in controlling the direction of functionally independent molecular pathways. Taken together, our data suggest that NAC1 serves as a potential molecular link between hormonal and developmental pathways that regulate the maturation process in post-embryonic root development.

(B) Proportion of plants with middle cortex in the WT, *mNAC1ox-4*, *35S::SCR-YFP*, and *35S::SCR-YFP/mNAC1ox-4*. The frequency of periclinal ACDs for middle cortex formation was analyzed at 7 dpg. n > 35 for each biological replicate; data represent mean ± SE of three biological replicates. Different letters above bars indicate a significant difference (one-way ANOVA, Tukey's multiple comparison test, $P < 0.05$).
(C) The numbers of periclinal cell divisions in the En of each plant that exhibited root middle cortex as shown in **(A)**; data represent mean ± SD. Individual values (black dots) are shown (n = 25). Different lowercase letters indicate significant differences by one-way ANOVA followed by Tukey's multiple comparison test ($P < 0.05$).
(D) qRT–PCR analysis showing the relative expression levels of *CYCD6;1* in the WT, *mNAC1ox-4*, *35S::SCR-YFP*, and *35S::SCR-YFP/mNAC1ox-4*. Total RNA was extracted from primary roots of 7-dpg seedlings. The expression level in the WT was set to "1." Three biological replicates with three technical replicates for each biological replicate were performed with similar results. Data represent mean ± SE of three biological replicates. Different letters above bars indicate a significant difference (one-way ANOVA, Tukey's multiple comparison test, $P < 0.05$).
(E) Confocal images of ACDs in roots of 7-dpg WT, *scr-2, mNAC1ox-4*, and *scr-2/mNAC1ox-4* seedlings. The insets illustrate periclinal ACDs that generate the En and middle cortex layers. The periclinal ACDs are indicated with white arrowheads. M, mutant cell layer. Scale bars, 50 μm.
(F) Proportion of plants with middle cortex in the WT, *scr-2*, *mNAC1ox-4*, and *scr-2/mNAC1ox-4*. The frequency of periclinal ACDs for middle cortex formation was analyzed at 7 dpg. n > 35 for each biological replicate; data represent mean ± SE of three biological replicates. Different letters above bars indicate a significant difference (one-way ANOVA, Tukey's multiple comparison test, $P < 0.05$).
(G) The number of periclinal cell divisions in the En of each plant that exhibited a root middle cortex as shown in **(E)**; data represent mean ± SD. Individual values (black dots) are shown (n = 25). Different lowercase letters indicate significant differences by one-way ANOVA followed by Tukey's multiple comparison test ($P < 0.05$).
(H) qRT–PCR analysis showing the relative expression levels of *CYCD6;1* in the WT, *scr-2*, *mNAC1ox-4*, and *scr-2/mNAC1ox-4*. Total RNA was extracted from primary roots of 7-dpg seedlings. The expression level in the WT was set to "1." Three biological replicates with three technical replicates for each biological replicate were performed with similar results. Data represent mean ± SE of three biological replicates. Different letters above bars indicate a significant difference (one-way ANOVA, Tukey's multiple comparison test, $P < 0.05$).
(I) NAC1, SCR, and TPL *trans*-repress *CYCD6;1* in *Arabidopsis* leaf protoplasts. The empty vector pBI221 was used as a negative control. Three biological replicates with three technical replicates for each biological replicate were performed with similar results. Data represent mean ± SE of three biological replicates. Different letters above bars indicate a significant difference (one-way ANOVA, Tukey's multiple comparison test, $P < 0.05$).
(J) Chromatin immunoprecipitation (ChIP)-qPCR results show the enrichment of NAC1 on the chromatin of *CYCD6;1*. Sonicated chromatin from 7-dpg seedlings (WT, *mNAC1ox-4*, *scr-2/mNAC1ox-4*, and *35S::SCR-YFP/mNAC1ox-4*) was precipitated with anti-MYC antibodies. The precipitated DNA was used as a template for qPCR analysis, with primers targeting different regions of *CYCD6;1*, as shown in Figure 2C. Three biological replicates with three technical replicates for each biological replicate were performed with similar results. Data represent mean ± SE of three biological replicates. $^{***}P < 0.001$, $^{**}P < 0.01$, $^{*}P < 0.05$, Student's *t* test.
(K) A proposed model for the regulation of middle cortex formation by the NAC1–TPL module through coordination with SCR and SHR. NAC1 plays a critical role in root ground tissue patterning, especially endodermal cell divisions, to form the middle cortex by directly repressing transcription of *CYCD6;1*. In WT roots, NAC1–TPL is required for accurate spatiotemporal repression of *CYCD6;1* expression. NAC1 and SCR directly interact and form an interdependent module to repress expression of the *CYCD6;1* gene in the En. NAC1 repels SHR from the promoter of *CYCD6;1*. In the *nac1* mutants, SHR is able to upregulate expression of *CYCD6;1*, promoting middle cortex formation.

Please cite this article in press as: Xie et al., NAC1 regulates root ground tissue maturation by coordinating with the SCR/SHR–CYCD6;1 module in *Arabidopsis*, Molecular Plant (2023), https://doi.org/10.1016/j.molp.2023.02.006

The frequency of periclinal cell divisions in the endodermis was significantly higher in *tpl mutants* than in *nac1* mutants, indicating that additional proteins besides NAC1 are required to link with TPL/TPR-mediated periclinal cell divisions in the endodermis. For instance, TPL/TPR-interacting transcriptional repressors play a key role in the signaling pathways of plant hormones such as auxin (Tiwari et al., 2004), jasmonate (Pauwels et al., 2010; Shyu et al., 2012), GA (Fukazawa et al., 2014), Abscisic Acid (Pauwels et al., 2010), brassinosteroids (Oh et al., 2014), salicylic acid (Arabidopsis Interactome Mapping Consortium, 2011), strigolactones (Jiang et al., 2013; Zhou et al., 2013), and ethylene (Arabidopsis Interactome Mapping Consortium, 2011). GA, Abscisic Acid, and ethylene signaling have been reported to participate in root middle cortex formation (Paquette and Benfey, 2005; Cui and Benfey, 2009a, 2009b; Lee et al., 2016). Whether TPL/TPR co-repressors interact with and are recruited by diverse hormone signaling pathways to regulate root middle cortex formation will be an interesting topic for future studies.

NAC1 has been shown to activate the expression of auxin-responsive genes via its C-terminal activation domain. Interestingly, we found that the N-terminal EAR motif in NAC1 is required for its interaction with the co-repressor TPL to negatively regulate the expression of *CYCD6;1*. NAC1 can function as either an activator or a repressor protein, depending on the nature of contextually recruited co-regulators in different developmental processes. This study reveals an unanticipated mechanism by which NAC1 recruits the co-repressor TPL to the *CYCD6;1* promoter and controls root ground tissue patterning through regulation of periclinal cell divisions in the endodermis.

METHODS

Plant material and growth conditions

All of the *Arabidopsis* mutants and/or transgenic lines used here are in the Col-0 background. The following have been described elsewhere: *cycd6;1* (Sozzani et al., 2010), *tpl-1* (the *tpl-1* mutation is a histidine substitution at asparagine 176 [N176H], and this allele acts as a dominant negative mutation for multiple TPR proteins; Long et al., 2006; Wang et al., 2013), *tpl-9* and *tpl-10* (two TPL T-DNA insertion mutants; Li et al., 2019), *scr-2* (Di Laurenzio et al., 1996), and *shr-2* (Helariutta et al., 2000). The T-DNA insertion lines *nac1-1* and *nac1-2* are from the Salk line described in the Arabidopsis Biological Resource Center (Columbus, OH, USA). The *nac1-1/cycd6;1* double mutant was obtained by crossing *nac1-1* and *cycd6;1*. The *nac1-1/scr-2* double mutant was obtained by crossing *nac1-1* and *scr-2*. The *nac1-1/shr-2* double mutant was obtained by crossing *nac1-1* with *shr-2*. The homozygous T-DNA mutant was identified by PCR using the primers on the T-DNA primer design website (http://signal.salk.edu/tdnaprimers.2.html). The primers are given in Supplemental Table 1. The *NAC1pro:gNAC1-GUS*, *CYCD6;1pro:GFP*, and *35S::SHR-GFP* transgenic plants have been described previously (Sozzani et al., 2010; Chen et al., 2016; Yu et al., 2017).

Prior to germination, seeds were surface sterilized by fumigation in chlorine gas and held for 2 days at 4°C on solidified half-strength Murashige and Skoog medium at a constant temperature of 22°C with a 16 h light/8 h dark photoperiod and a light intensity of 120 μmol photons m^{-2} s^{-1}. Roots of seedlings were examined at 5 or 7 dpg, depending on the experimental requirements.

Plasmid construction and plant transformation

Homozygous individuals were identified by PCR-based screening. The *mNAC1ox-2* and *mNAC1ox-4* constructs were created by introducing the *mNAC1* coding sequence (CDS) (Mallory et al., 2004; Guo et al., 2005) into the binary vector *pGWB18* and used for plant transformations. The *NAC1pro:NAC1* construct was generated by introducing the promoter region of *NAC1* and its genomic DNA into the binary vector *pGWB1* and used for plant transformations.

Constructs were transformed into *Agrobacterium tumefaciens* strain GV3101 to generate transgenic *Arabidopsis* plants using the floral-dip transformation method. Transformants were selected based on their resistance to hygromycin. Homozygous T3 or T4 lines were used to perform various experiments.

Microscopy and histochemical GUS staining

Root tips and GFP were imaged with LSM 900 and LSM 880 laser-scanning confocal microscopes (Carl Zeiss, Germany), respectively. The process was performed according to a method described previously (Ding and Friml, 2010).

To analyze middle cortex formation in the root endodermal layer, seedling roots were stained with propidium iodide (Sigma-Aldrich, 10 μg/ml in distilled water) and imaged with a confocal microscope. Quantitative analysis of the proportion of seedlings with periclinal cell divisions in the endodermis was performed.

For histochemical GUS staining, seedlings were infiltrated with 100 mM sodium phosphate buffer (pH 7.2), 0.1% Triton X-100, 2 mM potassium ferricyanide and potassium ferrocyanide, 10 mM EDTA, and 2 mM 5-bromo-4-chloro-3-indolyl-β-d-glucuronide and incubated at 37°C for 9 h. Samples were cleared in chloral hydrate and visualized with an Olympus BX53 microscope.

EMSA

The 1–199 amino acid sequence of *NAC1* was PCR amplified and cloned into the *pGEX-4T-1* vector. Then the Glutathione S-transferase-NAC1 protein (1–199 amino acids) was expressed in the *Escherichia coli* BL21 strain, and cells were grown to an optical density at 600 nm of ∼0.4–0.5. After induction with 0.2 mM Isopropyl-β-D-Thiogalactoside at 16°C overnight, cells were collected by centrifugation, washed once with PBS, and purified with glutathione Sepharose 4B (17-0756-01, GE Healthcare) according to the manufacturer's instructions. EMSA was performed using the LightShift Chemiluminescence EMSA Kit (20148, Thermo Fisher Scientific) according to the manufacturer's protocol.

ChIP-qPCR

DNA was harvested from 7-dpg seedlings of the WT and *mNAC1ox-4*; 7-dpg seedlings of the WT, *mNAC1ox-4*, *scr-2/mNAC1ox-4*, and *35S::SCR-YFP/mNAC1ox-4*; 7-dpg seedlings of the WT, *mNAC1ox-4*, and *mNAC1ox-4/35S::SHR-YFP*; and 7-dpg seedlings of the WT, *35S::SHR-YFP*, and *mNAC1ox-4/35S::SHR-YFP*. Tissue samples were crosslinked in 1× PBS containing 1% formaldehyde and placed under a vacuum for 15 min at room temperature. The ChIP procedure followed that described by Gendrel et al. (2005). The crosslinking reaction was stopped by addition of 125 mM glycine, and the tissue was placed under a vacuum for an additional 15 min. The tissue was rinsed twice with 40 ml 1× PBS, and as much 1× PBS as possible was removed by blotting. The crosslinked tissue was ground in liquid nitrogen, and 30 ml extraction buffer 1 (0.4 M sucrose, 10 mM Tris–HCl [pH 8.0], 10 mM $MgCl_2$, 5 mM β-mercaptoethanol, 0.1 mM PMSF, cocktail) was added. Nuclei were precipitated by centrifugation at 4000 *g* for 20 min, washed with 1 ml nuclear extraction buffer 2 (0.25 M sucrose, 10 mM Tris–HCl [pH 8.0], 10 mM $MgCl_2$, 1% Triton X-100, 5 mM β-mercaptoethanol, 0.1 mM PMSF, protease inhibitor cocktail). The resuspension was transferred and centrifuged at 12 000 *g* for 10 min. The supernatant was removed and resuspended in 300 μl extraction buffer 3 (1.7 M sucrose, 10 mM Tris–HCl [pH 8.0], 2 mM $MgCl_2$, 0.15% Triton X-100, 5 mM β-mercaptoethanol, 0.1 mM PMSF, cocktail). Nuclei were removed to a fresh tube with

Please cite this article in press as: Xie et al., NAC1 regulates root ground tissue maturation by coordinating with the SCR/SHR–CYCD6;1 module in *Arabidopsis*, Molecular Plant (2023), https://doi.org/10.1016/j.molp.2023.02.006

300 μl extraction buffer 3, centrifuged at 13 000 *g* for 1 h, and lysed in nucleus lysis buffer (50 mM Tris–HCl [pH 8.0], 10 mM EDTA [pH 8.0], 1% SDS, cocktail). Then the chromatin was sheared by sonication to an average size of approximately 200–400 bp, and antibodies recognizing the MYC tag (M047-11, MBL International, Japan) or GFP tag (D153-11, MBL International, Japan) were used. The immunoprecipitated chromatin complex was washed once with each of the following buffers in this order: low-salt buffer (20 mM Tris–HCl [pH 8.0], 2 mM EDTA, 150 mM NaCl, 1% Triton X-100, and 0.1% SDS), high-salt buffer (20 mM Tris–HCl [pH 8.0], 2 mM EDTA, 500 mM NaCl, 0.5% Triton X-100, and 0.2% SDS), LiCl buffer (10 mM Tris–HCl [pH 8.0], 1 mM EDTA, 0.25 M LiCl, 1% NP-40, and 0.5% sodium deoxycholate), and TE buffer (10 mM Tris–HCl [pH 8.0] and 1 mM EDTA). After washing, the immunoprecipitated chromatin was eluted with elution buffer (1% SDS and 0.1 M $NaHCO_3$). The protein–DNA crosslinks were reversed by incubating the immunoprecipitated complexes at 65°C overnight. The DNA was extracted with phenol/chloroform (1:1 [v/v]) and recovered by precipitation with ethanol in the presence of 0.3 M sodium acetate (pH 5.2) and 2 μl glycogen carrier (10 mg/ml). The samples were centrifuged at 13 000 *g* for 20 min at 4°C and resuspended in 40 μl RNase-free water. ChIP signals were quantified as the percentage of total input DNA and normalized relative to the control (*ACTIN2*). The quantities of precipitated DNA and input DNA were detected by qPCR. For the *CYCD6;1* promoter, primers were designed to amplify a ~70–150-bp fragment containing the NAC protein DNA-binding domain within the sequence upstream of the transcription start site. The enrichment in WT and transgenic plants was measured as a ratio of the bound promoter fragments over total input. The relevant primers are given in Supplemental Table 1.

Co-immunoprecipitation (CoIP) and western blotting

CoIP was performed according to a previous study (Lv et al., 2019; Yu et al., 2019). Mesophyll cells were harvested and lysed in cell lysis buffer (0.5 mM EDTA, 10 mM Tris–HCl [pH 7.5], 0.5% NP-40, 1 mM PMSF, and 150 mM NaCl) on ice for 30 min with pipetting every 10 min. Cell lysates were centrifuged, and the supernatant was incubated with MYC-Trap magnetic agarose beads (Chromotek, catalog number ytma-20) at 4°C for 2 h. The beads were washed three times with dilution buffer (10 mM Tris–HCl [pH 7.5], 150 mM NaCl, and 0.5 mM EDTA) and resuspended in SDS loading buffer. The resuspended beads were boiled for 10 min at 99°C, followed by western blotting with an anti-MYC (Abclonal, catalog number AE010) or anti-GFP (TransGen Biotech, catalog number HT801-02) antibody. For western blotting, protein was denatured and subjected to SDS-polyacrylamide gel electrophoresis (Bio-Rad) and transferred to polyvinylidene fluoride membranes (Millipore, catalog number IPVH00010). The membranes were blocked in 1× Tris buffered saline with Tween-20 with 5% milk for 2 h, immunoblotted with the indicated antibodies at 4°C overnight, and incubated for 2 h with horseradish peroxidase–conjugated secondary antibodies at room temperature. Blots were visualized with SuperSignal West Pico Luminol Enhancer Solution (Thermo Fisher Scientific).

Transient expression

The *NAC1*, *TPL*, *NAC1mEAR*, and *SCR* CDSs were amplified, and the resulting sequences were introduced into *pBI221* to place them under control of the CaMV 35S promoter. The *CYCD6;1* promoter sequences were amplified and introduced into the *pGreenII 0800-LUC* reporter vector. Both recombinant plasmids were then transferred into *Arabidopsis* protoplasts. Firefly luciferase and *Renilla* luciferase activities were measured using the Dual-Luciferase Reporter Assay System (www.promega.com). LUC activity was normalized against Renilla luciferase activity. Details of all primers used are given in Supplemental Table 1.

Split-luciferase complementation and BiFC assays

NAC1, TPL, SCR, or SHR was fused to the C or N terminus of YFP and transformed into *Agrobacterium* strain GV3101. *cYFP-TPL*, *nYFP-NAC1*, *cYFP-SCR*, *cYFP-SHR*, and *pSoup-P19* of *Agrobacterium* were cultivated overnight at 28°C, collected by centrifugation at 4000 *g* for 20 min, resuspended with Sodium Fatty Acid Methyl Ester sulfonate buffer (10 mM Sodium Fatty Acid Methyl Ester sulfonate, 10 mM $MgCl_2$, and 100 mM acetosyringone) to a final optical density 600 of ~1–1.5. Before infiltration into *N. benthamiana* leaves, equal volumes of *Agrobacterium* suspensions carrying the indicated constructs were incubated without light at 25°C for 3 h. *N. benthamiana* plants were left under long-day (16 h light/8 h dark), white-light conditions for 3 days after infiltration. The transfected leaves were grown at 25°C for 3 days before observation. The tobacco epidermal cells were then imaged under a Carl Zeiss LSM 800 confocal microscope. About 40 cells of 3 biological repetitions were analyzed in each combination. The combination with the empty vector was the negative control.

The split-luciferase complementation assay was performed as described in Chen et al. (2008) using NAC1-cLUC with TPL-nLUC, SCR-nLUC, or SHR-nLUC. SCR-cLUC with SHR-nLUC served as a positive control, and nLUC with NAC1-cLUC or cLUC and cLUC with SCR-nLUC, SHR-nLUC, or TPL-nLUC served as negative controls. Combinations of vectors were transformed into *N. benthamiana* leaves and expressed for 72 h, and images were captured with a charge-coupled device.

qRT–PCR

For qRT–PCR, RNA was isolated from roots using an RNeasy Plant Mini Kit (QIAGEN, Hilden, Germany) following the manufacturer's protocol. DNase I was used to remove contaminating genomic DNA, and a 2-μg aliquot was reverse transcribed using a Transcriptor First Strand cDNA Synthesis Kit (Roche, Basel, Switzerland) following the manufacturer's protocol. The subsequent qRT–PCRs were run on a MyiQ Real-Time PCR Detection System (Bio-Rad, Hercules, CA, USA) using FastStart Universal SYBR Green Master Mix (Roche, Basel, Switzerland). Each sample represents three biological replicates, and each biological replicate includes three technical replicates. *ACTIN2* (At3g18780) was used as the reference gene. Primers used for qRT–PCR are listed in Supplemental Table 1.

Yeast one-hybrid assay

The yeast one-hybrid assay was performed according to the manufacturer's manual for the Matchmaker One-Hybrid Library Construction and Screening Kit (www.clontech.com). The CDS of *NAC1* was inserted into the *pEntry* vector and into *pGADT7* by an LR reaction (Takara, USA). The target DNA sequence of the *CYCD6;1* promoter was inserted into the cloning site of the bait plasmid *pAbai*. Each of the constructs (including an empty vector as a control) was transferred separately into yeast Y1HGold using the Polyethylene glycol/Lithium Acetate method. After culturing on synthetic defined medium plates lacking Leu and Ura (SD−Leu−Ura) for 2 days, the transformants were transferred onto SD−Leu−Ura plates with different concentrations of Aureobasidin A (AbA) for analysis. Primers used for the yeast one-hybrid assay are listed in Supplemental Table 1.

Yeast two-hybrid assay

The yeast two-hybrid assay was performed according to the manufacturer's manual for the Matchmaker GAL4 Two-Hybrid System 3 (www.clontech.com). The CDSs of *TPL*, *SCR*, and *SHR* were inserted into the *pEntry* vector and then into *pGADT7* by an LR reaction (Takara, USA). The CDS of *NAC1* or *NAC1mEAR* was inserted into the cloning site of the bait plasmid *pGBKT7*. Each of the constructs (including an empty vector as a control) was transferred separately into yeast Y2HGold using the Polyethylene glycol/Lithium Acetate method. After culturing on synthetic defined medium plates lacking Trp and Leu (SD−Trp−Leu) for 2 days, the transformants were transferred onto SD−Trp−Leu−His plates for analysis. Primers used for the yeast two-hybrid assay are listed in Supplemental Table 1.

Please cite this article in press as: Xie et al., NAC1 regulates root ground tissue maturation by coordinating with the SCR/SHR–CYCD6;1 module in *Arabidopsis*, Molecular Plant (2023), https://doi.org/10.1016/j.molp.2023.02.006

Statistical analysis

We determined statistical significance by Student's *t*-test or one-way ANOVA with Tukey's multiple comparison test.

SUPPLEMENTAL INFORMATION

Supplemental information is available at *Molecular Plant Online*.

FUNDING

This work was supported by the National Natural Science Foundation of China (32170338 and 32061143005), Innovative Research Groups of Shandong University (2020QNQT014), and the Shandong Province Natural Science Foundation of the Major Basic Research Program (2017C03) (to Z.D.) and by the National Natural Science Foundation of China (32170311 and 31970192), the Shandong Province Funds for Excellent Young Scholars (ZR2020YQ19), and the Program of Shandong University Qilu Young Scholars (to X.K.).

AUTHOR CONTRIBUTIONS

Z.D. and X.K. conceived the study and designed the experiments. C.X., C.L., F.W., F.Z., J.L., J.W., and Z.D. performed the experiments and analyzed the data. C.X., X.Z., X.K., and Z.D. wrote the article. All authors discussed the results and commented on the article.

ACKNOWLEDGMENTS

We thank Prof. Qi Xie (University of Chinese Academy of Sciences), Prof. Shuang Wu (Fujian Agriculture and Forestry University), Prof. Lin Xu (Chinese Academy of Sciences), Prof. Lei Wang (Institute of Botany, the Chinese Academy of Sciences), and Prof. Yongxiu Liu (Institute of Botany, the Chinese Academy of Sciences) for sharing published materials. No conflict of interest is declared.

Received: July 27, 2022
Revised: January 4, 2023
Accepted: February 17, 2023

REFERENCES

Abrash, E.B., and Bergmann, D.C. (2009). Asymmetric cell divisions: a view from plant development. Dev. Cell **16**:783–796.

Aichinger, E., Kornet, N., Friedrich, T., and Laux, T. (2012). Plant stem cell niches. Annu. Rev. Plant Biol. **63**:615–636.

Aida, M., Ishida, T., Fukaki, H., Fujisawa, H., and Tasaka, M. (1997). Genes involved in organ separation in *Arabidopsis*: an analysis of the *cup-shaped cotyledon* mutant. Plant Cell **9**:841–857.

Arabidopsis Interactome Mapping Consortium. (2011). Evidence for network evolution in an *Arabidopsis* interactome map. Science **333**:601–607.

Baum, S.F., Dubrovsky, J.G., and Rost, T.L. (2002). Apical organization and maturation of the cortex and vascular cylinder in *Arabidopsis thaliana* (Brassicaceae) roots. Am. J. Bot. **89**:908–920.

Benfey, P.N., Linstead, P.J., Roberts, K., Schiefelbein, J.W., Hauser, M.T., and Aeschbacher, R.A. (1993). Root development in Arabidopsis: four mutants with dramatically altered root morphogenesis. Development **119**:57–70.

Benfey, P.N., and Scheres, B. (2000). Root development. Curr. Biol. **10**:R813–R815.

Bertolotti, G., Unterholzner, S.J., Scintu, D., Salvi, E., Svolacchia, N., Di Mambro, R., Ruta, V., Linhares Scaglia, F., Vittorioso, P., Sabatini, S., et al. (2021). A PHABULOSA-controlled genetic pathway regulates ground tissue patterning in the *arabidopsis* root. Curr. Biol. **31**:420–426.e6.

Boyer, F., and Simon, R. (2015). Asymmetric cell divisions constructing *Arabidopsis* stem cell niches: the emerging role of protein phosphatases. Plant Biol. **17**:935–945.

Causier, B., Ashworth, M., Guo, W., and Davies, B. (2012). The TOPLESS interactome: a framework for gene repression in Arabidopsis. Plant Physiol. **158**:423–438.

Chen, H., Zou, Y., Shang, Y., Lin, H., Wang, Y., Cai, R., Tang, X., and Zhou, J.M. (2008). Firefly luciferase complementation imaging assay for protein-protein interactions in plants. Plant Physiol. **146**:368–376.

Chen, X., Cheng, J., Chen, L., Zhang, G., Huang, H., Zhang, Y., and Xu, L. (2016). Auxin-independent *NAC* pathway acts in response to explant-specific wounding and promotes root tip emergence during de Novo root organogenesis in arabidopsis. Plant Physiol. **170**:2136–2145.

Cruz-Ramírez, A., Díaz-Triviño, S., Blilou, I., Grieneisen, V.A., Sozzani, R., Zamioudis, C., Miskolczi, P., Nieuwland, J., Benjamins, R., Dhonukshe, P., et al. (2012). A bistable circuit involving SCARECROW-RETINOBLASTOMA integrates cues to inform asymmetric stem cell division. Cell **150**:1002–1015.

Cui, H., and Benfey, P.N. (2009a). Interplay between SCARECROW, GA and LIKE HETEROCHROMATIN PROTEIN 1 in ground tissue patterning in the Arabidopsis root. Plant J. **58**:1016–1027.

Cui, H., and Benfey, P.N. (2009b). Cortex proliferation: simple phenotype, complex regulatory mechanisms. Plant Signal. Behav. **4**:551–553.

Cui, H., Levesque, M.P., Vernoux, T., Jung, J.W., Paquette, A.J., Gallagher, K.L., Wang, J.Y., Blilou, I., Scheres, B., and Benfey, P.N. (2007). An evolutionarily conserved mechanism delimiting SHR movement defines a single layer of endodermis in plants. Science **316**:421–425.

Di Laurenzio, L., Wysocka-Diller, J., Malamy, J.E., Pysh, L., Helariutta, Y., Freshour, G., Hahn, M.G., Feldmann, K.A., and Benfey, P.N. (1996). The *SCARECROW* gene regulates an asymmetric cell division that is essential for generating the radial organization of the Arabidopsis root. Cell **86**:423–433.

Ding, Z., and Friml, J. (2010). Auxin regulates distal stem cell differentiation in *Arabidopsis* roots. Proc. Natl. Acad. Sci. USA **107**:12046–12051.

Dinneny, J.R., and Benfey, P.N. (2008). Plant stem cell niches: standing the test of time. Cell **132**:553–557.

Fukazawa, J., Teramura, H., Murakoshi, S., Nasuno, K., Nishida, N., Ito, T., Yoshida, M., Kamiya, Y., Yamaguchi, S., and Takahashi, Y. (2014). DELLAs function as coactivators of GAI-ASSOCIATED FACTOR1 in regulation of gibberellin homeostasis and signaling in *Arabidopsis*. Plant Cell **26**:2920–2938.

Gallagher, K.L., Paquette, A.J., Nakajima, K., and Benfey, P.N. (2004). Mechanisms regulating SHORT-ROOT intercellular movement. Curr. Biol. **14**:1847–1851.

Gendrel, A.V., Lippman, Z., Martienssen, R., and Colot, V. (2005). Profiling histone modification patterns in plants using genomic tiling microarrays. Nat. Methods **2**:213–218.

Gong, X., Flores-Vergara, M.A., Hong, J.H., Chu, H., Lim, J., Franks, R.G., Liu, Z., and Xu, J. (2016). SEUSS integrates gibberellin signaling with transcriptional inputs from the SHR–SCR-SCL3 module to regulate middle cortex formation in the arabidopsis root. Plant Physiol. **170**:1675–1683.

Guo, H.-S., Xie, Q., Fei, J.-F., and Chua, N.-H. (2005). MicroRNA directs mRNA cleavage of the transcription factor *NAC1* to downregulate auxin signals for arabidopsis lateral root development. Plant Cell **17**:1376–1386.

Hegedus, D., Yu, M., Baldwin, D., Gruber, M., Sharpe, A., Parkin, I., Whitwill, S., and Lydiate, D. (2003). Molecular characterization of

Brassica napus NAC domain transcriptional activators induced in response to biotic and abiotic stress. Plant Mol. Biol. **53**:383–397.

Helariutta, Y., Fukaki, H., Wysocka-Diller, J., Nakajima, K., Jung, J., Sena, G., Hauser, M.T., and Benfey, P.N. (2000). The *SHORT-ROOT* gene controls radial patterning of the *Arabidopsis* root through radial signaling. Cell **101**:555–567.

Heo, J.-O., Chang, K.S., Kim, I.A., Lee, M.-H., Lee, S.A., Song, S.-K., Lee, M.M., and Lim, J. (2011). Funneling of gibberellin signaling by the GRAS transcription regulator scarecrow-like 3 in the *Arabidopsis* root. Proc. Natl. Acad. Sci. USA **108**:2166–2171.

Jiang, L., Liu, X., Xiong, G., Liu, H., Chen, F., Wang, L., Meng, X., Liu, G., Yu, H., Yuan, Y., et al. (2013). DWARF 53 acts as a repressor of strigolactone signalling in rice. Nature **504**:401–405.

Kagale, S., and Rozwadowski, K. (2011). EAR motif-mediated transcriptional repression in plants: an underlying mechanism for epigenetic regulation of gene expression. Epigenetics **6**:141–146.

Kikuchi, K., Ueguchi-Tanaka, M., Yoshida, K.T., Nagato, Y., Matsusoka, M., and Hirano, H.Y. (2000). Molecular analysis of the *NAC* gene family in rice. Mol. Gen. Genet. **262**:1047–1051.

Koizumi, K., Hayashi, T., and Gallagher, K.L. (2012a). SCARECROW reinforces SHORT-ROOT signaling and inhibits periclinal cell divisions in the ground tissue by maintaining SHR at high levels in the endodermis. Plant Signal. Behav. **7**:1573–1577.

Koizumi, K., Hayashi, T., Wu, S., and Gallagher, K.L. (2012b). The SHORT-ROOT protein acts as a mobile, dose-dependent signal in patterning the ground tissue. Proc. Natl. Acad. Sci. USA **109**:13010–13015.

Lee, S.A., Jang, S., Yoon, E.K., Heo, J.-O., Chang, K.S., Choi, J.W., Dhar, S., Kim, G., Choe, J.-E., Heo, J.B., et al. (2016). Interplay between ABA and GA modulates the timing of asymmetric cell divisions in the *arabidopsis* root ground tissue. Mol. Plant **9**:870–884.

Li, X., Chen, T., Li, Y., Wang, Z., Cao, H., Chen, F., Li, Y., Soppe, W.J.J., Li, W., and Liu, Y. (2019). ETR1/RDO3 regulates seed dormancy by relieving the inhibitory effect of the ERF12-TPL complex on delay of GERMINATION1 expression. Plant Cell **31**:832–847.

Long, J.A., Ohno, C., Smith, Z.R., and Meyerowitz, E.M. (2006). TOPLESS regulates apical embryonic fate in *Arabidopsis*. Science **312**:1520–1523.

Lv, B., Yu, Q., Liu, J., Wen, X., Yan, Z., Hu, K., Li, H., Kong, X., Li, C., Tian, H., et al. (2019). Non-canonical AUX/IAA protein IAA33 competes with canonical AUX/IAA repressor IAA5 to negatively regulate auxin signaling. EMBO J. **39**:e101515.

Mallory, A.C., Dugas, D.V., Bartel, D.P., and Bartel, B. (2004). MicroRNA regulation of NAC-domain targets is required for proper formation and separation of adjacent embryonic, vegetative, and floral organs. Curr. Biol. **14**:1035–1046.

Oh, E., Zhu, J.Y., Ryu, H., Hwang, I., and Wang, Z.Y. (2014). TOPLESS mediates brassinosteroid-induced transcriptional repression through interaction with BZR1. Nat. Commun. **5**:4140.

Ohta, M., Matsui, K., Hiratsu, K., Shinshi, H., and Ohme-Takagi, M. (2001). Repression domains of class II ERF transcriptional repressors share an essential motif for active repression. Plant Cell **13**:1959–1968.

Olsen, A.N., Ernst, H.A., Leggio, L.L., and Skriver, K. (2005). NAC transcription factors: structurally distinct, functionally diverse. Trends Plant Sci. **10**:79–87.

Ooka, H., Satoh, K., Doi, K., Nagata, T., Otomo, Y., Murakami, K., Matsubara, K., Osato, N., Kawai, J., Carninci, P., et al. (2003). Comprehensive analysis of NAC family genes in *Oryza sativa* and *Arabidopsis thaliana*. DNA Res. **10**:239–247.

Paquette, A.J., and Benfey, P.N. (2005). Maturation of the ground tissue of the root is regulated by gibberellin and SCARECROW and requires SHORT-ROOT. Plant Physiol. **138**:636–640.

Pauluzzi, G., Divol, F., Puig, J., Guiderdoni, E., Dievart, A., and Périn, C. (2012). Surfing along the root ground tissue gene network. Dev. Biol. **365**:14–22.

Pauwels, L., Barbero, G.F., Geerinck, J., Tilleman, S., Grunewald, W., Pérez, A.C., Chico, J.M., Bossche, R.V., Sewell, J., Gil, E., et al. (2010). NINJA connects the co-repressor TOPLESS to jasmonate signalling. Nature **464**:788–791.

Payankaulam, S., Li, L.M., and Arnosti, D.N. (2010). Transcriptional repression: conserved and evolved features. Curr. Biol. **20**:R764–R771.

Riechmann, J.L., Heard, J., Martin, G., Reuber, L., Jiang, C., Keddie, J., Adam, L., Pineda, O., Ratcliffe, O.J., Samaha, R.R., et al. (2000). *Arabidopsis* transcription factors: genome-wide comparative analysis among eukaryotes. Science **290**:2105–2110.

Scheres, B. (2007). Stem-cell niches: nursery rhymes across kingdoms. Nat. Rev. Mol. Cell Biol. **8**:345–354.

Scheres, B., Di Laurenzio, L., Willemsen, V., Hauser, M.T., Janmaat, K., Weisbeek, P., and Benfey, P.N. (1995). Mutations affecting the radial organisation of the Arabidopsis root display specific defects throughout the embryonic axis. Development **121**:53–62.

Shyu, C., Figueroa, P., Depew, C.L., Cooke, T.F., Sheard, L.B., Moreno, J.E., Katsir, L., Zheng, N., Browse, J., and Howe, G.A. (2012). JAZ8 lacks a canonical degron and has an EAR motif that mediates transcriptional repression of jasmonate responses in *Arabidopsis*. Plant Cell **24**:536–550.

Sozzani, R., Cui, H., Moreno-Risueno, M.A., Busch, W., Van Norman, J.M., Vernoux, T., Brady, S.M., Dewitte, W., Murray, J.A.H., and Benfey, P.N. (2010). Spatiotemporal regulation of cell-cycle genes by SHORTROOT links patterning and growth. Nature **466**:128–132.

Ten Hove, C.A., and Heidstra, R. (2008). Who begets whom? Plant cell fate determination by asymmetric cell division. Curr. Opin. Plant Biol. **11**:34–41.

Tiwari, S.B., Hagen, G., and Guilfoyle, T.J. (2004). Aux/IAA proteins contain a potent transcriptional repression domain. Plant Cell **16**:533–543.

van den Berg, C., Willemsen, V., Hage, W., Weisbeek, P., and Scheres, B. (1995). Cell fate in the *Arabidopsis* root meristem determined by directional signalling. Nature **378**:62–65.

van den Berg, C., Willemsen, V., Hendriks, G., Weisbeek, P., and Scheres, B. (1997). Short-range control of cell differentiation in the *Arabidopsis* root meristem. Nature **390**:287–289.

Wang, L., Kim, J., and Somers, D.E. (2013). Transcriptional corepressor TOPLESS complexes with pseudoresponse regulator proteins and histone deacetylases to regulate circadian transcription. Proc. Natl. Acad. Sci. USA **110**:761–766.

Xie, C., and Ding, Z. (2022). NAC1 maintains root meristem activity by repressing the transcription of E2Fa in arabidopsis. Int. J. Mol. Sci. **23**:12258.

Xie, Q., Frugis, G., Colgan, D., and Chua, N.H. (2000). *Arabidopsis* NAC1 transduces auxin signal downstream of TIR1 to promote lateral root development. Genes Dev. **14**:3024–3036.

Yu, Q., Li, P., Liang, N., Wang, H., Xu, M., and Wu, S. (2017). Cell-Fate specification in arabidopsis roots requires coordinative action of lineage instruction and positional reprogramming. Plant Physiol. **175**:816–827.

Yu, Z., Zhang, D., Xu, Y., Jin, S., Zhang, L., Zhang, S., Yang, G., Huang, J., Yan, K., Wu, C., and Zheng, C. (2019). CEPR2 phosphorylates and

accelerates the degradation of PYR/PYLs in Arabidopsis. J. Exp. Bot. **70**:5457–5469.

Zhang, X., Zhou, W., Chen, Q., Fang, M., Zheng, S., Scheres, B., and Li, C. (2018). Mediator subunit MED31 is required for radial patterning of *Arabidopsis* roots. Proc. Natl. Acad. Sci. USA **115**:E5624–E5633.

Zhang, Z.L., Ogawa, M., Fleet, C.M., Zentella, R., Hu, J., Heo, J.O., Lim, J., Kamiya, Y., Yamaguchi, S., and Sun, T.P. (2011). Scarecrow-like 3 promotes gibberellin signaling by antagonizing master growth repressor DELLA in Arabidopsis. Proc. Natl. Acad. Sci. USA **108**:2160–2165.

Zhou, F., Lin, Q., Zhu, L., Ren, Y., Zhou, K., Shabek, N., Wu, F., Mao, H., Dong, W., Gan, L., et al. (2013). D14-SCF^{D3}-dependent degradation of D53 regulates strigolactone signalling. Nature **504**:406–410.

Zhou, W., Lozano-Torres, J.L., Blilou, I., Zhang, X., Zhai, Q., Smant, G., Li, C., and Scheres, B. (2019). A jasmonate signaling network activates root stem cells and promotes regeneration. Cell **177**:942–956.e14.